# PHOSPHORYLATION AND UBIQUITINATION REGULATE PROTEIN PHOSPHATASE 5 ACTIVITY AND ITS PROSURVIVAL ROLE IN KIDNEY CANCER

**Author: Natela Dushukyan**

**A Dissertation in Biochemistry and Molecular Biology**

Submitted in partial fulfillment of the requirements for the Master of Science degree in the College of Graduate Studies of State University of New York, Upstate Medical University.

Approved_____
(Sponsor's Signature)

Date_____

# Table of Contents

# Acknowledgements

I want to thank my great mentor Dr. Mehdi Mollapour for his support, motivation, and his guidance. His enthusiasm and passion for his research made my time in his lab, not only incredibly educational, but also memorable and enjoyable. I also want to thank Dr. Dimitra Bourboulia for her support and advice. I have learned a lot over the past two years about what it means to be a good scientist, and could not have had better examples than Dr. Mollapour and Dr. Bourboulia.

I consider myself lucky to have spent my time in a wonderful work environment of people who support each other, and who are always ready for a laugh. And for that great lab atmosphere I must thank my labmates Mark Woodford and Rebecca Sager, and also the members of Dr. Bourboulia's lab: Alexander Baker-Williams and Javier Sanchez-Pozo. Likewise I want to thank previous lab member Dr. Diana Dunn, and all of the volunteers, rotation students, and medical residents that I had the pleasure to work with throughout my time in the lab.

Likewise, I would like to thank Dr. Gennady Bratslavsky for his support and for providing the patient tumor samples that allowed me to do translational research with strong clinical relevance.

I want to thank all of the members of my thesis committee: Dr. Mehdi Mollapour, Dr. Dimitra Bourboulia, and Dr. Xin Jie Chen for making time for me.

In addition, I would like to acknowledge my funding sources: SUNY Upstate Medical University, the College of Graduate Studies, Upstate Foundation, One Square Mile of Hope Foundation, Carol M. Baldwin Breast Cancer Fund, the Urology Care Foundation Research Scholar Award Program, and the American Urological Association.

I especially want to thank my parents and my brother for their support of my goals, for their patience, and for the motivation they tirelessly provided over the past two years. Lastly, I would like to thank all the friends I made here for always finding ways to make me laugh and for being there for me.

# Abstract

Protein Phosphatase 5 (PP5) is a serine/threonine phosphatase known to regulate many essential cellular functions including steroid hormone signaling, stress response, proliferation, apoptosis, and DNA repair. PP5 is a known co-chaperone of the molecular chaperone heat shock protein 90 (Hsp90), and its regulation of Hsp90 aids with the proper activation of Hsp90 clients and with steroid hormone signaling. Hsp90 is also one of the strongest activators of PP5, as it releases the auto-inhibition of PP5 by interacting with the N- terminal tetratricopeptide repeat (TPR) domain of PP5. Our lab has recently shown that PP5 is phosphorylated at T362, and that this phosphorylation acts as an "on switch" resulting in the hyperactivation of PP5. Misregulation of this key phosphatase has been shown to aid in the tumor progression of ER-dependent and independent breast cancer. Elevated PP5 levels have also been linked to colorectal cancer, hepatocellular carcinoma (HCC), lymphoma, and prostate cancer.

The work presented here reveals the pro-survival role that PP5 plays in kidney cancer. Clear cell renal cell carcinomas (ccRCC) are most often driven by mutations in the von Hippel-Lindau tumor suppressor (VHL). The data in this thesis shows that VHL binds and multi mono-ubiquitinates PP5 at two lysine residues K185 and K199. This post-translational modification negatively regulates PP5 like an "off switch" and ultimately leads to its degradation by the proteasome. Mutations in the *VHL* gene that result in inactive mutants or a lack of VHL protein expression lead to ccRCC tumors. The data in this thesis shows that these VHL-*null* tumors become dependent on elevated levels of PP5, and that both PP5 knockdown and inhibition lead to cancer cell death. The data further shows that the decrease in PP5 activity in VHL-null cells results in the induction of the extrinsic

apoptotic pathway with a dramatic increase in the cleavage of PARP and caspases 3, 7, and 8.

# List of Figures

# List of Tables

# Chapter 1 - General Introduction

## 1.1 Protein Phosphatase 5

Regulation of cellular processes and signaling networks in cells often occurs by phosphorylation and dephosphorylation of key proteins. Normal levels of phosphorylation are maintained by the balance of kinases and phosphatases (Ardito et al., 2017; Cohen, 2001; Meeusen and Janssens, 2018). When the activity of kinases and phosphatases is altered through inhibition, activation, or mutation, their ability to properly regulate the phosphorylation levels of their substrates is compromised. This leads to misregulation and abnormal activity of their substrates and, in turn, misregulation of key signaling pathways responsible for cell survival. As a result, misregulation of kinases and phosphatases leads to many diseases including many different cancers, myotonic muscular dystrophy, Williams syndrome, Coffin-Lowry syndrome and many others (Ardito et al., 2017; Cohen, 2001; Meeusen and Janssens, 2018). Studying the function and regulation of kinases and phosphatases is therefore of paramount importance for the development of treatments for these diseases. Protein phosphatase 5 (PP5) is a serine/threonine phosphatase that helps regulate cellular functions such as stress response, proliferation, apoptosis, and DNA repair (Hinds and Sanchez, 2008). PP5 has been shown to increase proliferation in most cells, and has also been directly linked to the progression of breast cancer (Hinds and Sanchez, 2008). The role of PP5 in proliferation makes it an important subject for research and also a promising target for cancer treatment.

PP5 is part of the phosphoprotein phoshatases (PPP) family which also includes PP1, PP2A, PP2B, PP4, PP6, and PP7 (Shi, 2009; Swingle et al., 2004). Unlike other members of its family, PP5 has very low levels of basal activity due to the fact that it is auto-inhibited (Figures 1A and 1B) (Yang et al., 2005). PP5 is also different from the other

six PPP family members as it is the only one to be encoded by a single gene. The PPP5c gene is located on chromosome 19 and is about 2kb in length (Xu et al., 1996).

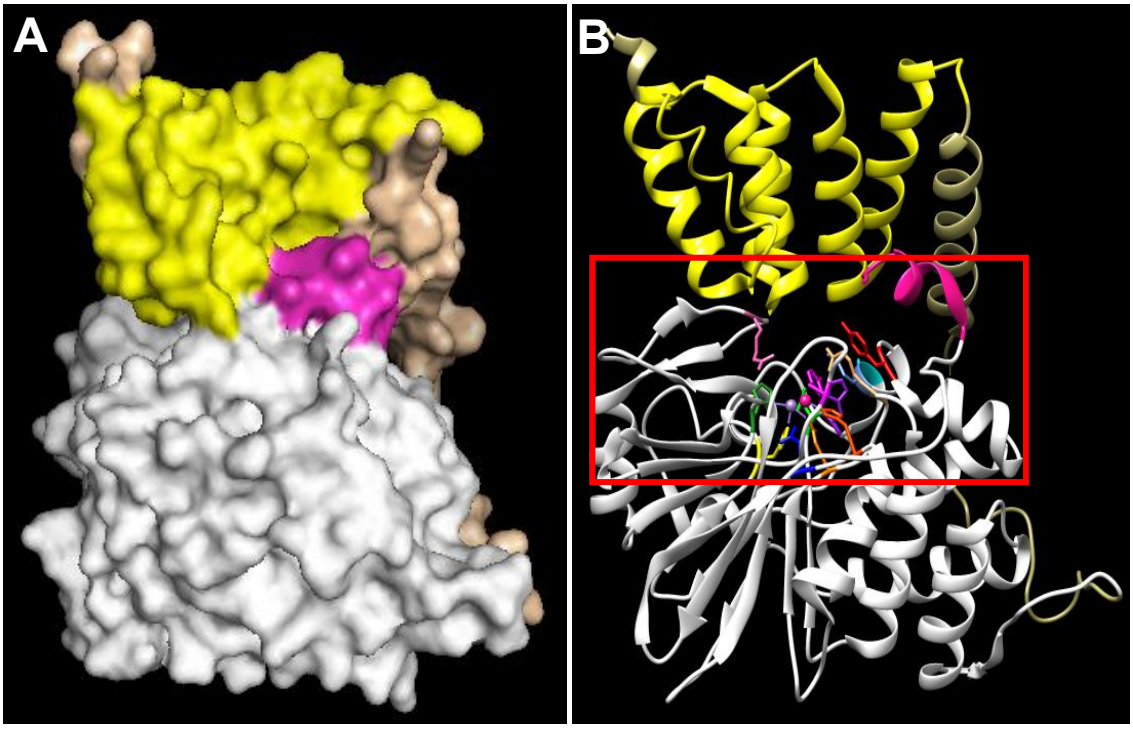


**Figure 1: Structure of auto-inhibited PP5.**

**(A)** Space fill model of PP5. Tetratricopeptide repeat TPR (yellow); αJ helix (purple); catalytic domain (white).
**(B)** Ribbon model with key catalytic residues highlighted.

Interestingly, PP5 is also the only PPP member that is a single polypeptide, as most of the other members of the family (PP1, PP2A, PP2B, and PP4) are comprised of two or more proteins that are encoded by different genes that are responsible for various functions such as regulation and catalysis. These multi-polypeptide proteins are held together mostly through weak non covalent interactions (Swingle et al., 2004; Yang et al., 2005). On the other hand, like other members of its family, PP5 is a metal-dependent protein phosphatase as it requires the coordination of two metal ions within its catalytic site for activity (Golden et al., 2008b; Swingle et al., 2004)

## 1.2 PP5 Structure and Function

As mentioned above, the structure of PP5 is unique amongst PPP members. PP5 has three consecutive tetratricopeptide repeat (TPR) motifs in the N terminal domain (shown in yellow in figures 1A and 1B), starting at residue 28 and ending at 129 (Das et al., 1998). The TPR domain is responsible for the regulation of PP5 activity, and is essential for both auto-inhibition and activation. This N-terminal TPR domain interacts with a specific C-terminal alpha J helix (αJ) (shown in purple in figures 1A and 1B) to block substrate access to the catalytic groove, which results in a closed and auto-inhibited PP5 conformation. However, the TPR domain is also crucial for PP5 interactions with activators such as heat shock protein 90 (Hsp90), and fatty acids like arachidonic acid (Vaughan et al., 2008; Yang et al., 2005; Zeke et al., 2005). The interactions between these activators and the TPR domain result in the disruption of interactions between the TPR domain and the inhibitory αJ helix. This allows PP5 to change to an open and active conformation giving substrates sufficient access to the catalytic site.

Within the catalytic site of PP5 there are several key residues that are essential for activity. Also essential is the presence of two metal ions. PP5 has been shown to coordinate $Mn^{+2}$, $Zn^{+2}$, and $Fe^{+2}$, but commonly prefers $Mn^{+2}$ (Oberoi et al., 2016; Swingle et al., 2004). These two metal ions are important for coordinating the target phosphate groups of PP5 substrates. The ions likewise interact with two water molecules in the catalytic site and are also likely responsible for the nucleophilic attack by metal-ligated water, which is the most likely of three mechanisms proposed for the mechanism of PPP family proteins (Swingle et al., 2004). The two metal ions are each coordinated by six ligands. Of those six ligands, two (D271 and water 1) are shared by the metal ions. The four remaining ligands

for each ion are as follows: metal 1 ($M^1$) is coordinated by D242, H244, water 2, and $O^1$ (oxygen from substrate's phosphate group), and $M^2$ is coordinated by N303, H352, H427, and $O^2$ (Swingle et al., 2004). Each metal ion interacts with one oxygen atom of the substrate phosphate group while residues D242 and H352 balance that interaction on the opposite side of $M^1$ and $M^2$, respectively (Figure 2A). The remaining metal-coordinating residues all form bonds in one plane, giving both $Mn^{+2}$ ions an octahedral geometry.

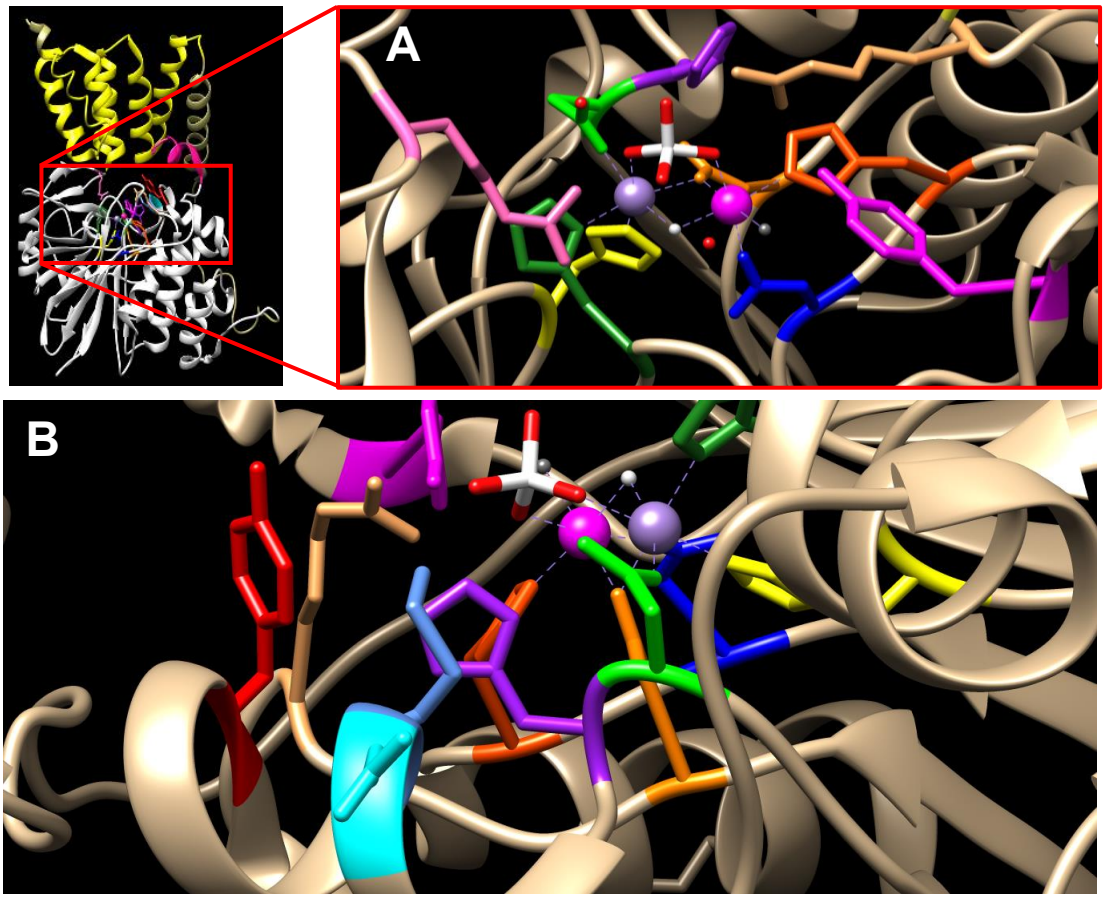


**Figure 2: Catalytic domain contacts of PP5.**

**(A)** Catalytic domain metal contacts. metal 1 ($M^1$) (magenta sphere) coordinated by: D271 (orange); water 1 (light gray); D242 (blue); H244 (red orange); water 2 (dark gray), and $O^1$ (oxygen from substrate's phosphate group) (red). $M^2$ (indigo) coordinated by: N303 (neon green); H352 (yellow); H427 (forest green), and $O^2$ (red). R400 (pink) interacts with substrates**.**
**(B)** Substrate contacts: R275 (tan); N303 (neon green); H304 (purple); N308 (cyan); M309 (light blue); Y313 (red); and Y451 (magenta).

These residues are all important for the maintenance of proper PP5 activity, but they are far from the only key residues within the catalytic domain of PP5. Residues R275, N303, H304, and R400 are all responsible for the coordination of the target phosphate ion through direct hydrogen bond interactions with all four oxygen atoms of the phosphate group (Figure 2A and 2B). N303 interacts with both $M^2$ and the substrate phosphate group, while the other residues are set slightly above the metal ions and only interact with the substrate (Figure 3). Interestingly, though D274 does not have any direct interaction with

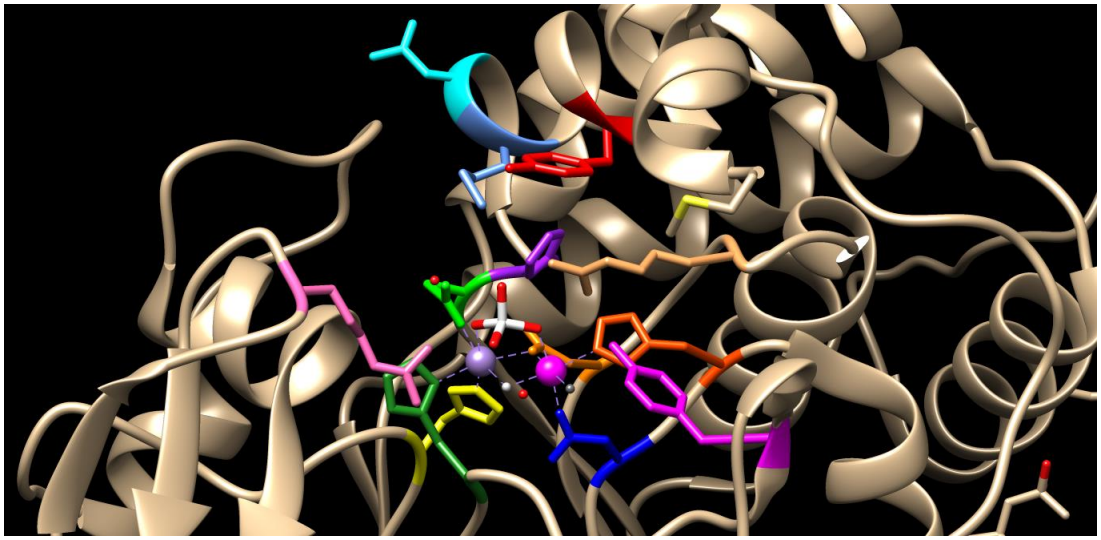

**Figure 3: Catalytic domain of PP5 with bound substrate.**

View of catalytic domain with substrate and all key residues highlighted. Colors as in **(2A)** and **(2B).**

the metal ions, water, or substrates, it is critical for PP5 activity because it forms a necessary hydrogen bond with H304 (Swingle et al., 2004). These residues are all essential for PP5 activity.

In addition to the aforementioned residues, there are more crucial residues that are important for PP5 function, and they are N308, M309, Y313, and Y451. Of these four residues, the first three are involved in coordinating PP5 substrates through direct coordination (N308 and Y313), or through van der Waals interactions (M309). The last

residue (Y451) does not directly interact with substrates, but instead forms hydrogen bonds with R275 and a water molecule that help determine substrate conformation. Other residues contributing to the determination of substrate conformation include N308, Y313, and R400 (Vaughan et al., 2008). The substrate contacting residues essentially form a lining along the inside of the catalytic pocket above the metal ions ensuring the proper, and stable, positioning of PP5 substrates (Figure 3).

Although the catalytic domains of PP5 and other PPP proteins are similar enough to be inhibited by the same molecule such as okadaic acid, the abundance of key residues that are unique to PP5 make it druggable (Golden et al., 2008b; Hinds and Sanchez, 2008). Developing a specific PP5 inhibitor is an enticing concept as it would allow us to regulate many different cellular pathways, and would also provide a possible treatment for breast cancer.

### 1.3 PP5 substrates and binding partners

PP5 is known to play a regulatory role in many signaling and stress response pathways and, as such, has been shown to interact with many different proteins that are key regulators of various signaling pathways ranging from steroid hormone receptors to tumor suppressors. PP5 is known to interact with the GR- Hsp90 heterocomplex, and help regulate GR signaling (Table 1) (Davies et al., 2005; Jacob et al., 2015). It has also been shown to directly interact, and co-localize, with CDC16/CDC27 subunits of the anaphase-promoting complex (APC) (Ollendorff and Donoghue, 1997). This data suggests that PP5 may play an important role in the regulation of APC activity, and thus in the cell's progression from metaphase into anaphase. In addition, PP5 has been reported to regulate

p53 through upstream pathways showing that PP5 also plays a role in DNA damage response (Amable et al., 2011; Zuo et al., 1998).

**Table 1: Proteins with known interactions with PP5.**

| Substrates | Activators | In Complex |
|---|---|---|
| Cdc37 | Hsp90 | G α12 |
| GR | CK1δ | G α13 |
| ER α and β | Rac1 | Erk 1/2 |
| Raf1 | Copine I | PP2A |
| Ask1 | | eIF2 α |
| DNA-PKcs | | ATM |
| Tau | | CDC16 |
| CK1ε | | CDC27 |
| | | ATR |
| | | Hsf1 |
| | | AR |
| | | Cryptochrome 2 |

Other known interactions include: CK1ε (Partch et al., 2006); copine (Tomsig et al., 2003); cryptochrome 2 (Zhao and Sancar, 1997); Hsp90-dependent heme-regulated eIF2α kinase (Shao et al., 2002); apoptosis signal-regulating kinase 1 (ASK1) (Morita et al., 2001); DNA-PKcs (DNA-dependent Ser/Thr protein kinase) (Wechsler et al., 2004); ATM (ataxiatelangiectasia mutated kinase) (Ali et al., 2004); ATR (ATM and Rad 3 related kinase) (Zhang et al., 2005); A-regulatory subunit of protein phosphatase type 2A (Lubert et al., 2001); G12-α/G13-α subunits of heterotrimeric G proteins (Yamaguchi et al., 2002); Rac1 and Ras (Gentile et al., 2006; Mazalouskas et al., 2014); and Raf1 (von Kriegsheim et al., 2006). Through these interactions, PP5 helps regulate many different pathways and checkpoints involved in the cell cycle, varying from DNA damage checkpoints to the transition to anaphase, and to apoptosis. As free PP5 is usually auto-inhibited, many of

these PP5 interactions occur in complex with Hsp90, as Hsp90 is a strong activator of PP5 activity.

## 1.4 Co-chaperone function of PP5

The interaction between PP5 and Hsp90 is likely the most well studied of all PP5 protein interactions. The N-terminal PP5 TPR domain binds to the C-terminal MEEVD TPR-binding domain of Hsp90 (Haslbeck et al., 2015; Silverstein et al., 1997). This interaction releases the auto-inhibition of PP5, activating its phosphatase activity. As a result, PP5 acts as a co-chaperone to regulate the rate of the Hsp90 chaperone cycle by dephosphorylating another Hsp90 co-chaperone Cdc37 at S13 (Figure 4) (Vaughan et al., 2008). This allows for the activation of Cdc37 and, in turn, the activation of Hsp90 kinase clients (Golden et al., 2008b). This regulation helps determine the speed with which Hsp90 moves through its cycle, and affects the ability of Hsp90 to chaperone kinase clients. Hypoactive PP5 mutations that cannot effectively dephosphorylate Cdc37 trap kinase clients in the Hsp90-Cdc37-PP5 complex. The trapped complex results in a slowed down chaperone cycle that stabilizes generally transient interactions with kinases, allowing them to be co-immunoprecipitated with PP5. In contrast, wild-type and hyperactive PP5 mutants maintain transient interactions and do not co-immunoprecipitate kinase clients (Oberoi et al., 2016).

Interestingly, both hypoactive and hyperactive PP5 mutants affect the binding of Hsp90 to its inhibitors. The hypoactive mutants show a dose dependent increase of Hsp90 binding to geldanamycin, whereas the hyperactive mutant increases drug binding in a dose independent manner (Oberoi et al., 2016). The increase in Hsp90 drug binding with

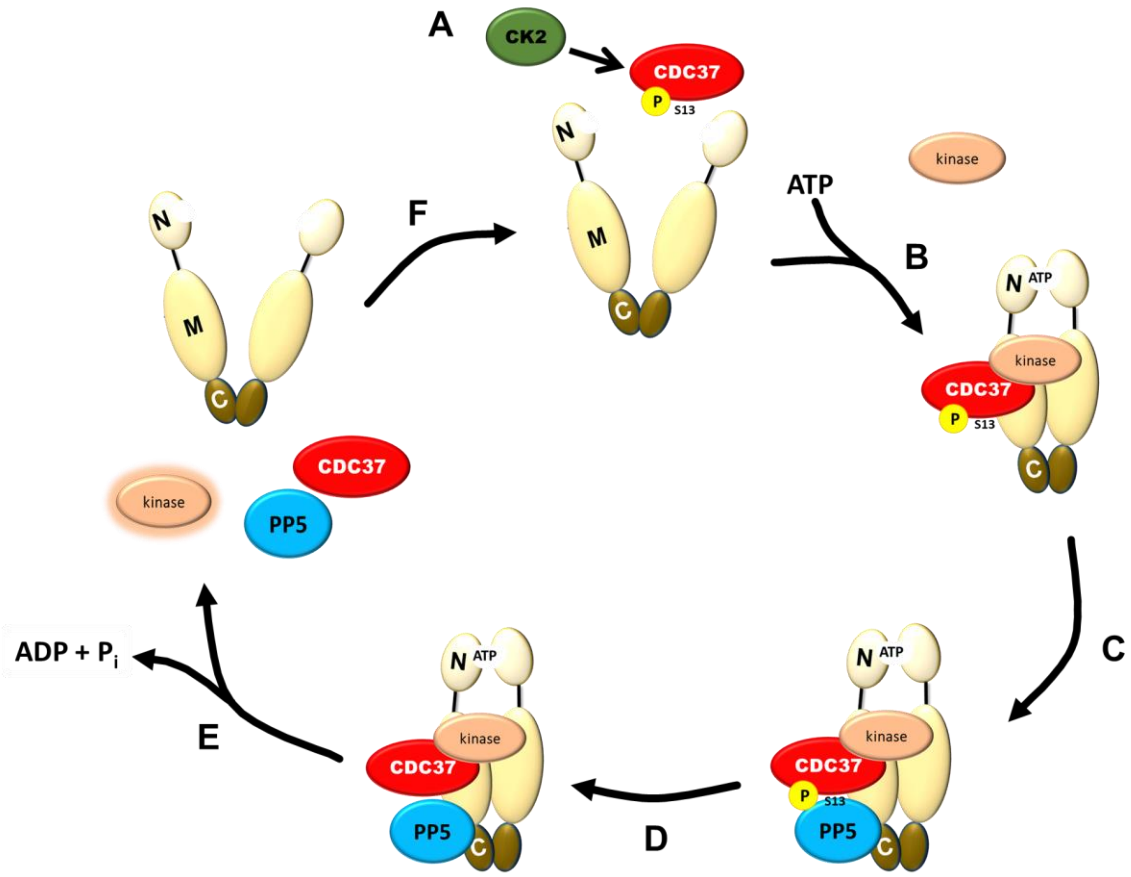


**Figure 4: Activation of Hsp90 kinase clients by the Hsp90-Cdc37-PP5 chaperone complex.**

**(A)** CK2 phosphorylates Cdc37 at S13, allowing Cdc37 to bind its kinase client. Hsp90 is in its open conformation without any clients or co-chaperones bound.
**(B)** ATP binds to the N-terminal domain of Hsp90, resulting in a closed Hsp90 conformation. Phosphorylated Cdc37 with its kinase client binds to the closed ATP-bound conformation of Hsp90.
**(C)** PP5 binds to the C-terminal domain of Hsp90, activating its phosphatase activity.
**(D)** PP5 dephosphorylates *bona fide* substrate Cdc37 at S13 resulting in the activation of Cdc37, and subsequent activation of the kinase client. Hsp90 hydrolyzes ATP allowing it to activate the kinase client.
**(E)** PP5, Cdc37, and the active kinase are released from the complex. ADP and $P_i$ are released from the N domain, allowing Hsp90 to return to an open, unbound conformation.
**(F)** Unbound Hsp90 is free to repeat its chaperone cycle.

hypoactive PP5 is likely due to the fact that hypoactive PP5 traps Hsp90 with its clients, essentially locking it in a bound conformation that seems to have a higher affinity for drugs. Hyperactive PP5, on the other hand, allows for a faster chaperone cycle which means that Hsp90 will change from an unfavorable conformation to a more favorable conformation

faster. As a result, the drug can bind Hsp90 more effectively in the presence of mutant PP5 than it does in the presence of the wild-type. PP5 activity is therefore a key factor in determining the affinity of Hsp90 for its inhibitors.

PP5 does not only help Hsp90 chaperone kinase clients, but also helps Hsp90 chaperone steroid hormone receptors like glucocorticoid receptor (GR) (Schopf et al., 2017). PP5 dephosphorylates GR at three N-terminal serine residues (S203, S211, and S226) and, as a result, acts as a regulator of GR transcriptional activity. Decrease in PP5 activity through both pharmacological inhibition and down-regulation results in increased levels of phosphorylation at all three aforementioned serine residues (Bouazza et al., 2012; Wang et al., 2007; Zhang et al., 2009). The ratio of phosphorylation levels of all three residues determines the activity of GR, and PP5 maintains different ratios of serine phosphorylation under different circumstances to ensure proper GR signaling. In addition to GR, PP5 has been found in complex with estrogen receptor (ER). This interaction leads to the dephosphorylation of ER at S118, and this dephosphorylation results in decreased ER transcriptional activity (Ikeda et al., 2004; Sanchez, 2012). PP5 has also been shown to dephosphorylate peroxisome proliferator-activated receptor-gamma (PPARγ) at S112. In PP5 knockout MEFs, PPARγ-S112 does not get dephosphorylated. As a result, PPARγ is unable to induce expression of pro-adipogenic genes. The same study in PP5 knockout mice has also shown that PP5 mediates bone loss induced by rosiglitazone (Stechschulte et al., 2016). PP5 thus plays an essential role in the regulation of steroid hormone signaling as part of its regulation of Hsp90 chaperone activity.

## 1.5 PP5 Role in Cancer

### 1.5.1 Elevated PP5 levels in breast cancer

PP5 levels have been found to be elevated in breast cancer, which is often linked to the activity of ERα, a substrate of PP5. The presence of ERα in mammary tumors of transgenic mice resulted in the development of tumors 6 months earlier than in mice lacking ERα (Yue et al., 2013). However, despite the lack of ERα, the mice still developed tumors, verifying that ERα is not always necessary for breast cancer formation or progression. In ER dependent breast cancers, the presence of estrogen stimulates ER leading the activation of pro-survival pathways, and in some cases the activation of oncogenes. However, in ER independent breast cancers, estrogen does not overstimulate ERα. Instead estrogen, or its metabolites, can have direct genotoxic effects that result in oncogenic mutations (Fernandez et al., 2006; Liehr, 2000; Yue et al., 2013). As there are ER dependent and independent breast cancers, it is possible that PP5 may play a different role in each one.

A study conducted in a mouse xenograft model observed a correlation between constitutive PP5 overexpression and an increase in tumor growth rate. This correlation was confirmed with the observation that PP5 overexpression in MCF-7 cells led to increased proliferation and protection from cell death (Golden et al., 2008a). This coincides with the finding that estrogen can stimulate the expression of PP5 (Sanchez, 2012). Interestingly, there is also somewhat conflicting data showing that PP5 dephosphorylation of ER at S118 has been shown to decrease ER transcription of some estrogen responsive genes (Ikeda et al., 2004). These data imply a possible negative feedback loop in which estrogen increases levels of PP5, allowing PP5 to negatively regulate ER activity. This regulatory mechanism

may be used in the formation and proliferation of ER independent breast cancers that may require high levels of PP5 for other signaling pathways. Another possible explanation is that PP5 overexpression in breast cancer is independent of its regulation of ER, and is instead dependent on increased estrogen levels (Zhang et al., 2009). If that is the case, then breast cancer cells might require high levels of PP5 for other pathways that can overcome the detrimental loss of ER transcription that results from PP5 overexpression. Unfortunately, the specific role of PP5 in breast cancer is not yet fully understood, and more research is needed to elucidate the precise crosstalk between PP5 signaling complexes and estrogen.

### 1.5.2 Elevated PP5 protein levels in cancers

PP5 has also been linked to several other cancers including colorectal, hepatocellular carcinoma (HCC), and lymphoma. One study in 2014 showed that silencing PP5 in RKO and SW1116 colorectal cancer cells leads to decreased cell proliferation; G0/G1 cell cycle arrest; and increased apoptosis (Wang et al., 2015). These results were obtained by silencing PP5 with lentiviral shRNA and performing a methylthiazol tetrazolium assay (MTT), colony formation assay, and flow cytometry. Though the role of PP5 in colorectal cancer growth is not fully known, these results show that colorectal cancer cells are dependent on PP5 for survival. In contrast, another study conducted in colorectal cancer cells showed that overexpression of PP5 in HT-29 cells led to increased sensitivity to mTOR inhibitor Way-600. This sensitivity was found to be dependent on PP5-mediated dephosphorylation of DNA-PKcs at T2609 (Wu et al., 2015). Together these results show that PP5 is necessary for colorectal cancer growth, but that it can also play an anti-

tumorigenic role through DNA-PKcs dephosphorylation when it is overexpressed. Further research is required to elucidate the nuances of the role PP5 plays in colorectal cancer.

A more recent study in 2017 likewise linked PP5 to liver cancer (Chen et al., 2017). In this study patient samples of hepatocellular carcinoma tumors showed elevated PP5 levels when compared to adjacent normal tissue. Additionally, high PP5 expression was linked to a significantly lower progression-free survival rate in HCC patients, further validating the tumorigenic role of PP5 in liver cancer. In HCC cells, PP5 overexpression led to increased cancer cell proliferation and colony formation, while PP5 knockdown resulted in significant cancer cell death (Chen et al., 2017). Therefore, PP5 is necessary for the survival and progression of liver cancer, and inhibition of PP5 in liver cancer may prove to be a promising method of cancer treatment.

In a study of 6 lymphoma patient samples, 4 showed PP5 levels that were more than 1.3 times higher than in normal tissue (Ghobrial et al., 2005). Though the authors did not choose to further study the effect of higher PP5 levels, their finding does show a possible link between PP5 and lymphomas. A similar link exists between PP5 and prostate cancer, as PP5 levels are elevated in prostate cancer cell lines when compared to normal prostate cell lines (Periyasamy et al., 2007). Although this link has not been thoroughly studied, immunoprecipitation of either PP5 or androgen receptor yields co-immunoprecipitation of the other, which shows that there is some interaction between PP5 and AR (Schulke et al., 2010). While no studies have shown PP5 dephosphorylating AR, that is likely due to the lack of research into this interaction (Periyasamy et al., 2007; Schulke et al., 2010). AR associates with many of the same TPR containing proteins that compete with PP5 for GR binding, which strengthens the likelihood that there is an as-of-yet undiscovered regulatory

interaction between AR and PP5 (Schulke et al., 2010). Given the interaction of PP5 with AR, it is possible that PP5 might play a role in prostate cancer.

PP5 is a crucial phosphatase that regulates many cellular functions including steroid hormone signaling, stress response, proliferation, apoptosis, and DNA repair (Hinds and Sanchez, 2008). As a co-chaperone of Hsp90, PP5 works in complex with Hsp90 and its clients to regulate cell signaling pathways that are crucial for cell survival and growth (Vaughan et al., 2008). PP5 has been shown to increase proliferation in most cells, and misregulation of PP5 activity has been directly linked to the progression of breast cancer (Golden et al., 2008a). The link between elevated PP5 levels and tumor growth has also been established in liver cancer, lymphoma, and prostate cancer (Chen et al., 2017; Ghobrial et al., 2005; Schulke et al., 2010). The evidence clearly demonstrates that PP5 plays a significant role in the survival and propagation of cancer cells, thus making the development of a PP5 inhibitor a promising avenue for cancer research. Though there are several naturally occurring PP5 inhibitors, none are specific for PP5. Further research into the understanding of PP5 and its activation is, therefore, of paramount importance. Such knowledge can lead to the development of inhibitors that may be able to treat not just breast cancer, but potentially other cancers that overexpress, and become dependent on, PP5.

# Chapter 2 - Phosphorylation and Ubiquitination Regulate Protein Phosphatase 5 Activity and Its Prosurvival Role in Kidney Cancer

**Natela Dushukyan**[1,2,3,8], Diana M. Dunn[1,2,3,8], Rebecca A. Sager[1,2,3], Mark R. Woodford[1,2,], David R. Loiselle[4], Michael Daneshvar[1,2], Alexander J. Baker-Williams[1,2,3], John D. Chisholm[5], Andrew W. Truman[6], Cara K. Vaughan[7], Timothy A. Haystead[4], Gennady Bratslavsky[1,2], Dimitra Bourboulia[1,2,3], Mehdi Mollapour[1,2,3,9†]

[1] Department of Urology,

[2] Upstate Cancer Center,

[3] Department of Biochemistry and Molecular Biology, SUNY Upstate Medical University, 750 E. Adams St., Syracuse, NY 13210, USA

[4] Department of Pharmacology and Cancer Biology, Duke University Medical Center, Durham, NC 27710, USA.

[5] Department of Chemistry, Syracuse University, 1-014 Center for Science and Technology, Syracuse, NY 13244, USA

[6] Department of Biological Sciences, University of North Carolina at Charlotte, Charlotte, NC 28223, USA

[7] Institute of Structural and Molecular Biology, University College London and Birkbeck College, Biological Sciences, Malet Street, London, WC1E 7HX, UK

[8] These authors contributed equally

[9] Lead Contact



**Full citation:** Dushukyan, N., Dunn, D.M., Sager, R.A., Woodford, M.R., Loiselle, D.R., Daneshvar, M., Baker-Williams, A.J., Chisholm, J.D., Truman, A.W., Vaughan, C.K., et al. (2017). Phosphorylation and Ubiquitination Regulate Protein Phosphatase 5 Activity and Its Prosurvival Role in Kidney Cancer. Cell Rep 21, 1883-1895.

**Declaration:** The experiments presented in this chapter were conducted by Natela Dushukyan unless otherwise stated in figure legends.

## 2.1 Introduction

The serine/threonine protein phosphatase-5 (PP5) regulates multiple cellular signaling networks. A number of cellular factors, including Hsp90 promote the activation of PP5. As such, the majority of PP5 substrates are in complex with Hsp90 and include the glucocorticoid receptor (GR), tumor suppressor p53, and the co-chaperone Cdc37 (Vaughan et al., 2008; Zuo et al., 1998; Zuo et al., 1999). PP5 also functions as a co-chaperone of Hsp90 (Haslbeck et al., 2015; Vaughan et al., 2008; Wandinger et al., 2006; Xu et al., 2012) and its dephosphorylation of Cdc37 in complex with Hsp90 activates kinase clients. Hsp90 and its co-chaperones are also subject to post-translational modifications (PTMs) (reviewed here: (Mayer and Le Breton, 2015; Walton-Diaz et al., 2013; Woodford et al., 2016a)) that regulate their activity.

However, it is unclear whether post-translational modifications also influence PP5 phosphatase activity. This thesis shows an "on/off switch" mechanism for PP5 regulation. The casein kinase-1 δ (CK1δ) phosphorylates T362 in the catalytic domain of PP5, which activates and enhances phosphatase activity independent of Hsp90. Overexpression of the phosphomimetic T362E-PP5 mutant hyper-dephosphorylates substrates such as the co-chaperone Cdc37 and the glucocorticoid receptor in cells. Our proteomic approach identified the tumor suppressor von Hippel-Lindau protein (VHL) to interact and ubiquitinate K185/K199-PP5 for proteasomal degradation in a hypoxia- and prolyl hydroxylation-independent manner. Finally, *VHL*-deficient clear cell renal cell carcinoma (ccRCC) cell lines and patient tumors exhibit elevated PP5 levels. Down-regulation of PP5 causes ccRCC cells to undergo apoptosis, suggesting a pro-survival role for PP5 in kidney cancer.

## 2.2 Results

### 2.2.1 CK1δ phosphorylates T362 in the catalytic domain of PP5

Previous work has shown that PP5 interacts with casein kinase 1 (CK1) (Partch et al., 2006). We used this information and showed that human CK1δ interacts with human PP5. Amino-terminal FLAG-tagged PP5 (PP5-FLAG) was transiently expressed in HEK293 cells. Using anti-FLAG M2 affinity gel, PP5-FLAG was immunoprecipitated and co-immunoprecipitation of CK1δ was observed by immunoblotting (Figure 5A). A similar

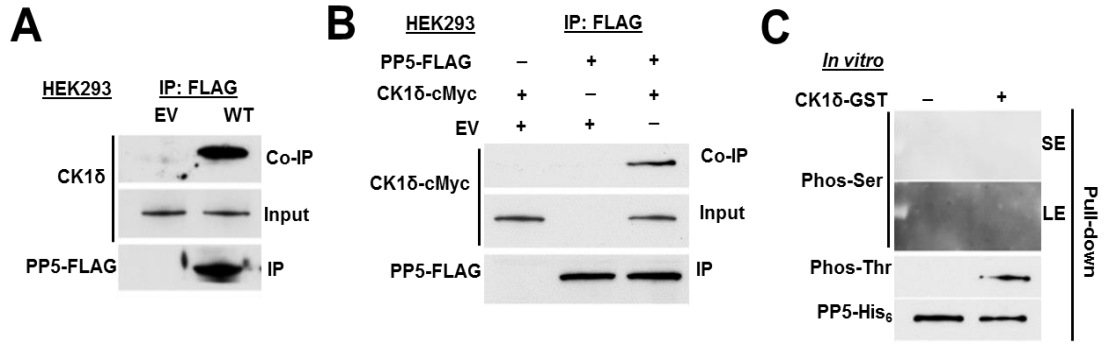


**Figure 5. CK1δ phosphorylates PP5.**

**(A)** Empty vector (EV) or PP5-FLAG plasmids were transiently expressed and immunoprecipitated (Vaughan et al.) from HEK293 cells. Co-immunoprecipitation (Co-IP) of endogenous CK1δ was examined by immunoblotting. Empty vector (EV) was used as a control.
**(B)** PP5-FLAG and CK1δ-cMyc were transiently co-expressed in HEK293 cells. PP5-FLAG was IP and Co-IP of CK1δ-cMyc was assessed by immunoblotting. Empty vector (EV) was used as a control.
**(C)** Recombinant PP5-His6 was used in an in vitro kinase assay. CK1δ-GST phosphorylates only threonine residues on PP5-His6. Phosphorylation was examined by immunoblotting with anti-phosphoserine or phosphothreonine antibodies. SE (short exposure) and LE (long exposure) of the radiographic film. Results presented in this figure were obtained by former graduate student Diana Dunn.

experiment was also conducted by transiently co-transfecting HEK293 cells with PP5-FLAG and N-terminally cMyc-tagged CK1δ. Immunoprecipitation of PP5-FLAG led to co-immunoprecipitation of CK1δ-cMyc (Figure 5B). These data show that human CK1δ interacts with PP5 in mammalian cells.

Previous work from my current lab has shown that PP5-mediated dephosphorylation of the co-chaperone Cdc37 is essential for activation of the kinase clients of Hsp90 (Vaughan et al., 2008). My lab examined if CK1δ directly phosphorylates PP5 in an *in vitro* kinase assay. Bacterially expressed and purified PP5-$His_6$ was bound to Ni-NTA agarose and then incubated with active CK1δ-GST (glutatione S-transferase). Using immunoblotting and anti-phosphothreonine-P6623 (Sigma-Aldrich) antibody, it was possible to detect threonine phosphorylation of PP5 (Figure 5C). Unlike in yeast, CK1δ does not phosphorylate any serine sites on PP5 (Figure 5C). There are seven mammalian CK1 isoforms, however CK1δ and CK1ε display the highest homology (Schittek and Sinnberg, 2014).

Generally, the CK1 consensus phosphorylation site is S/Tp-X-X-S/T, where S/Tp refers to phospho-serine or phospho-threonine priming sites, X refers to any amino acid, and the underlined residues refer to the target site (Flotow et al., 1990). Our group did not identify any possible threonine phosphorylation site using this consensus motif in PP5. CK1 also phosphorylates a related unprimed site, D/E-X-X-S/T, where underlined residues refer to the phosphorylated amino acid (Flotow et al., 1990). We identified five PP5 threonine residues within this CK1 consensus site (Figure 6A); T33, T121, T171, T238 and T362. With the exception of T238, all the identified threonine sites are located on the surface of PP5, and of the surface residues, only one (T362) is located in the catalytic domain (Figures 6A and 6B). These sites were individually mutated to non-phosphorylatable alanine in the PP5-FLAG construct and transiently co-expressed with or without CK1δ-cMyc in HEK293 cells. PP5-FLAG was then immunoprecipitated with anti-FLAG M2 affinity gel and threonine phosphorylation was detected by immunoblotting

using anti-phosphothreonine-P6623 (Sigma-Aldrich) antibody. Overexpression of CK1δ-cMyc increased threonine phosphorylation of wild-type PP5-FLAG and the non-phosphorylatable threonine mutants except for T362A-PP5-FLAG (Figure 6C). The threonine phosphorylation of this mutant was significantly lower, even with overexpression of CK1δ-cMyc (Figure 6C), suggesting that T362 is phosphorylated by CK1δ.

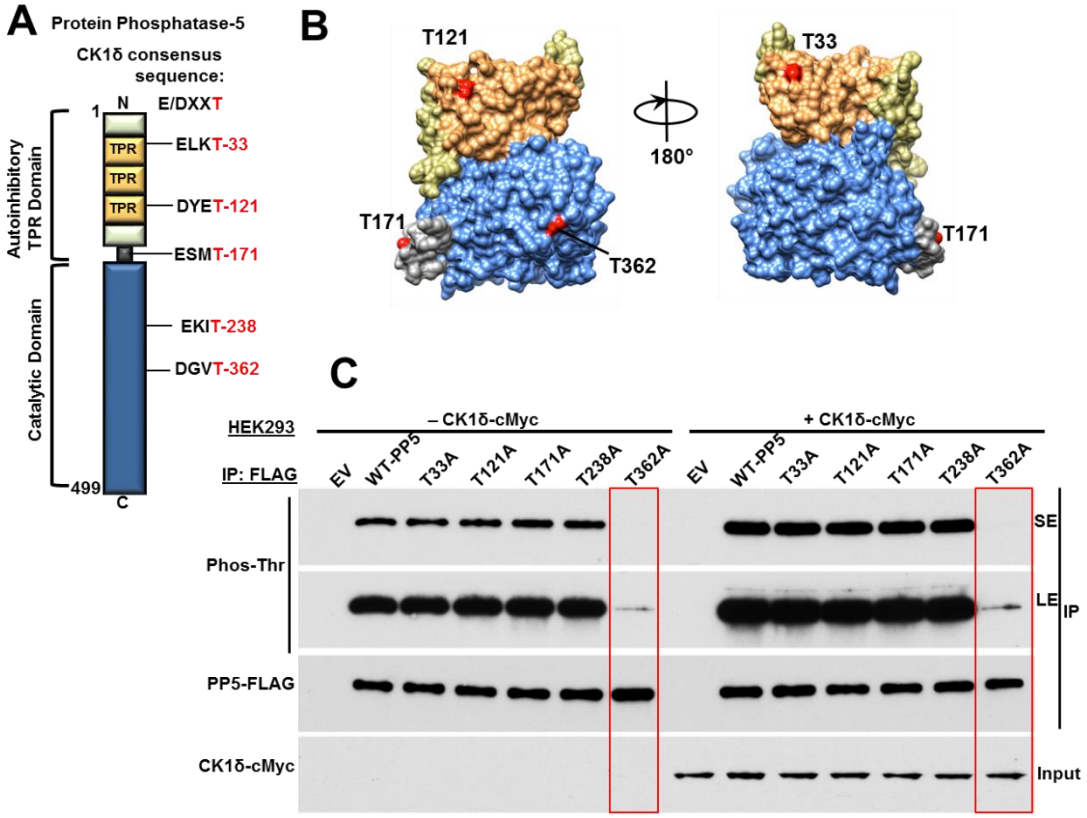


**Figure 6. PP5 Phosphorylation at T362.**

**(A)** Schematic representation of PP5 with highlighted CK1δ consensus sequence E/DXXT.
**(B)** Potential CK1δ targeted threonine sites on PP5 are highlighted on the cartoon of representation of the PP5 protein, modeled with UCSF Chimera software (PDB:1WAO). Color-coded as in Figure 2A.
**(C)** PP5-threonine residues within the CK1δ consensus sequence were mutated individually to alanine (A), transiently expressed, and IP from HEK293 cells. Threonine phosphorylation was detected by immunoblotting with anti-phosphothreonine antibody. This experiment was repeated with co-transfection of CK1δ-cMyc with the phospho-PP5-FLAG mutants in HEK293 cells. PP5-FLAG and its mutants were isolated and threonine phosphorylation was assessed by immunoblotting with anti-phosphothreonine antibody. SE (short exposure) and LE (long exposure) of the radiographic film. Results presented in this figure were obtained by former lab member Diana Dunn.

### 2.2.2 T362 phosphorylation activates and increases PP5 activity independent of Hsp90

To determine the impact of T362 phosphorylation on the activation and activity of PP5, we initially tested the ability of the T362-PP5 phospho-mutants to dephosphorylate para-nitrophenyl phosphate (pNPP), a commonly used small molecule for assaying nonspecific phosphatase activity (Oberoi et al., 2016). Our data showed that the bacterially expressed and purified wild-type-PP5-$His_6$ had basal phosphatase activity and addition of Hsp90α stimulated this activity (Figures 7A and 7B). The phosphomimetic T362E-PP5-$His_6$ or CK1δ mediated phosphorylation of T362-PP5-$His_6$ stimulated PP5 activity in the absence of Hsp90α (Figures 7A and 7B). We then repeated the same experiments but instead used the non-phosphorylatable T362A-PP5-$His_6$. This mutant had a similar basal phosphatase activity as the wild-type-PP5-$His_6$ suggesting that the mutation did not structurally affect the PP5 activity. However, the addition of Hsp90α or CK1δ (attempting to phosphorylate T362A-PP5-$His_6$ *in vitro*) did not stimulate the phosphatase activity (Figures 7A and 7B).

We next used an *in vitro* dephosphorylation assay of phospho-S13-Cdc37, which is a *bona fide* substrate of PP5 (Vaughan et al., 2008). We first showed that addition of Hsp90α to wild-type PP5 leads to complete dephosphorylation of phospho-S13-Cdc37 after 30 minutes (Figures 8A and 8B). However, addition of Hsp90α to phosphomimetic T362E-PP5-$His_6$ (Figure 8A) or phospho-T362-PP5-$His_6$ (Figure 8B) led to dephosphorylation of Cdc37 after only 10 min. To determine whether activation of phospho-T362-PP5 is independent of Hsp90, we repeated the above experiment in the absence of Hsp90α. Our data revealed that wild-type PP5 is unable to dephosphorylate phospho-S13-Cdc37 in the absence of Hsp90α (Figures 8C and 8D). However, the

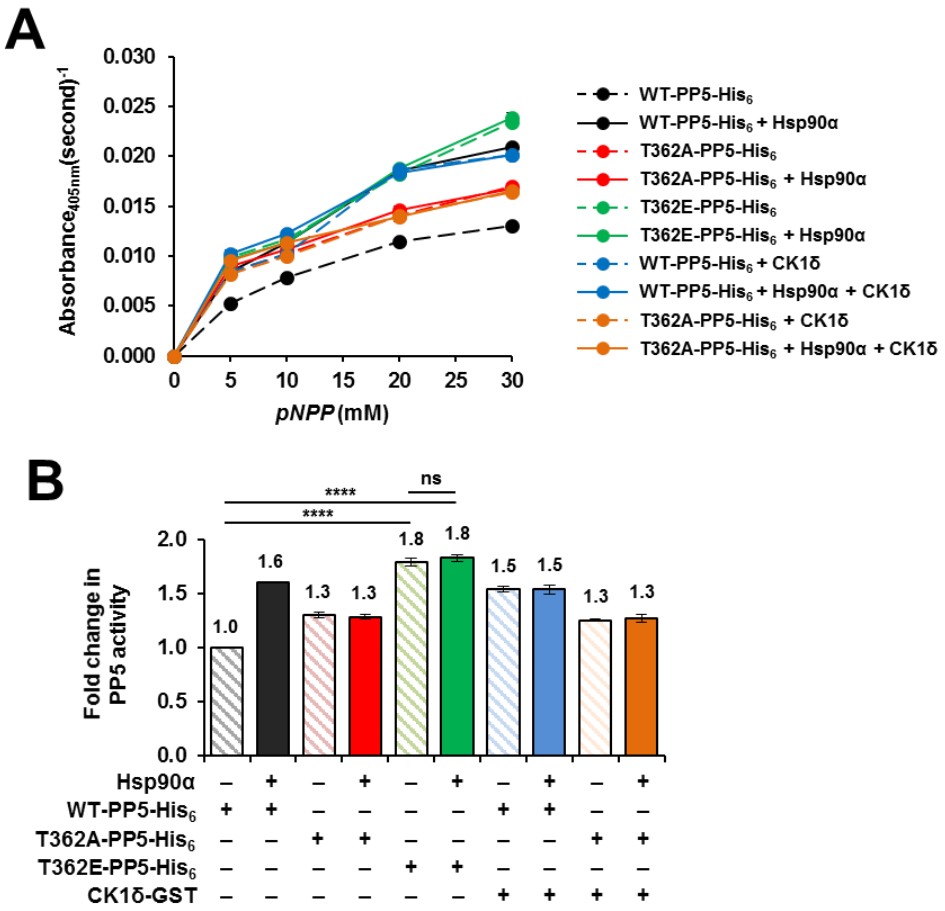


**Figure 7. Phosphatase activity of the phospho-T362-PP5.**

**(A)** Rate of dephosphorylation of the model substrate pNPP by the wild-type PP5 (Ashkenazi et al.) and PP5 mutants: T362A (red), T362E (green), CK1δ mediated phosphorylation of the wild-type PP5 (blue), and CK1δ mediated phosphorylation of the T362A (orange). The data represents three independent experiments.
**(B)** Fold increase from wild-type PP5 basal activity at 30 mM data point from samples in (A). The error bars represent mean ± S.D. of three independent experiments. A Student's t-test was performed to assess statistical significance (****P<0.0001) or non-significant (n.s.)). Results presented in this figure were obtained by former graduate student Diana Dunn.

phosphomimetic T362E-PP5-His$_6$ (Figure 8C) or CK1δ phosphorylated T362-PP5 (Figure 8D) dephosphorylated phospho-S13-Cdc37 *in vitro* even in the absence of Hsp90.

To ascertain whether CK1δ interaction with PP5 caused an increase in its phosphatase activity, CK1δ was incubated with PP5-His$_6$ in the presence and absence of ATP. CK1δ has the ability to interact with PP5-His$_6$ independent of ATP (Figure 8E).

However, only CK1δ incubation with PP5-$His_6$ in the presence of ATP results in PP5 activation. Indicating that PP5 is only activated after CK1δ mediated phosphorylation of PP5. This activation leads to dephosphorylation of PP5 substrate, (i.e. phospho-S13-Cdc37) (Figure 8F). Taken together, these *in vitro* data suggest that CK1δ mediated phosphorylation of T362-PP5 causes activation and hyperactivity of PP5 phosphatase independent of binding to Hsp90.

To obtain further evidence in support of this conclusion, we overexpressed wild-type PP5-FLAG and the phospho-mutants T362A and T362E in HEK293 cells. The dephosphorylation of PP5 substrates, phospho-S13-Cdc37 and phospho-S211-glucocorticoid receptor (GR), were examined by immunoblotting. Overexpression of wild-type PP5-FLAG led to dephosphorylation of phospho-S13-Cdc37 and phospho-S211-GR (Figure 8G). This effect was enhanced with overexpression of the phosphomimetic T362E-PP5-FLAG and unaffected (similar to the empty vector control) with T362A-PP5-FLAG, which is consistent with our *in vitro* data (Figure 8G). Finally, we confirmed that the interaction of the phospho-T362 mutants with Hsp90, Cdc37 and GR were not affected, and therefore our observation is not due to lack of interaction of PP5 mutants with the substrates (Figure 8H). Our *in vitro* and *in vivo* data here show that phosphorylation of T362-PP5 is involved in both activation and hyperactivity of PP5 (Figure 9). Furthermore, based on our *in vitro* results, CK1δ mediated phosphorylation and activation of PP5 does not depend on binding to Hsp90.

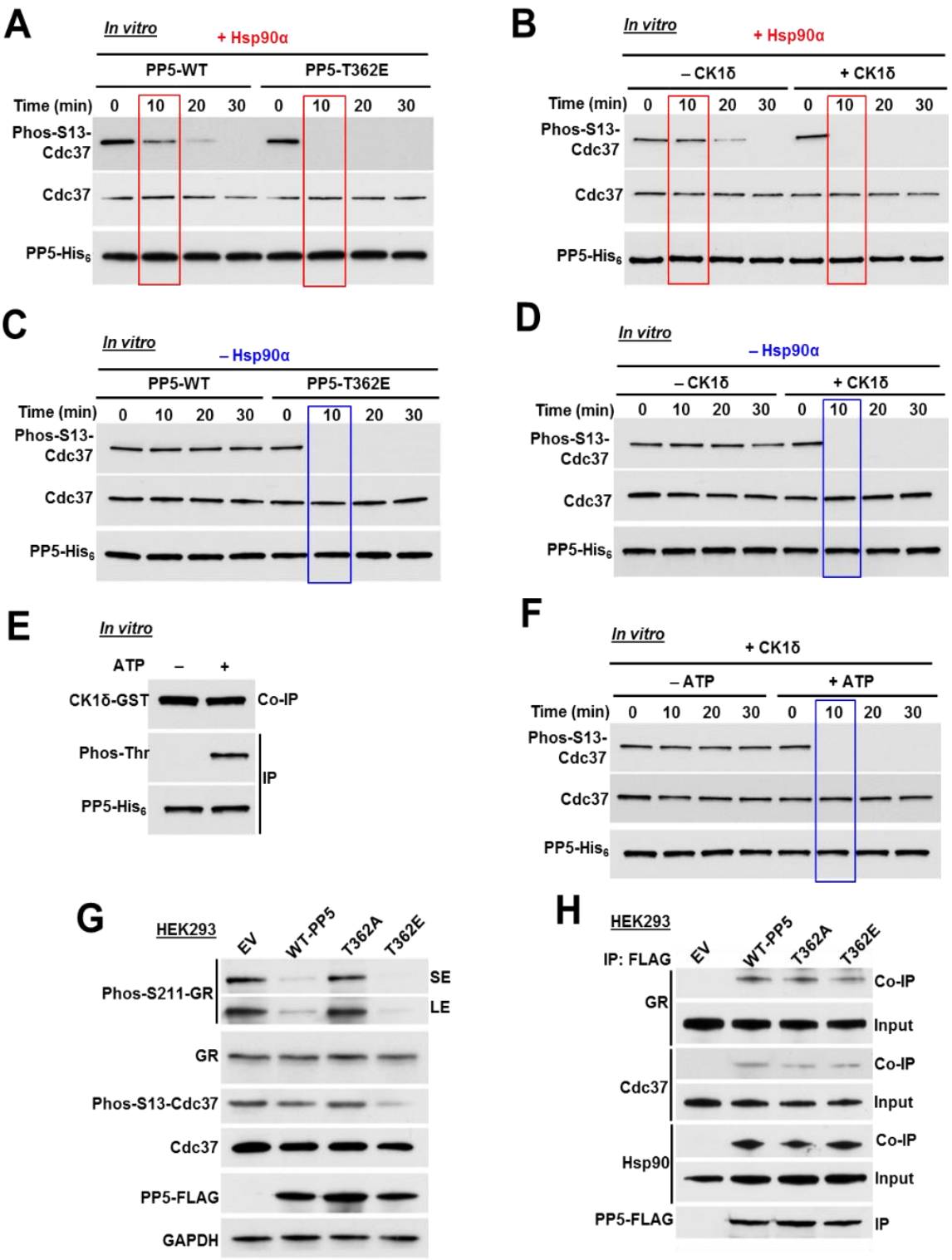
A
In vitro
+ Hsp90α
PP5-WT
PP5-T362E
Time (min) 0 10 20 30 0 10 20 30
Phos-S13-Cdc37
Cdc37
PP5-His6
B
In vitro
+ Hsp90α
– CK1δ
+ CK1δ
Time (min) 0 10 20 30 0 10 20 30
Phos-S13-Cdc37
Cdc37
PP5-His6
C
In vitro
– Hsp90α
PP5-WT
PP5-T362E
Time (min) 0 10 20 30 0 10 20 30
Phos-S13-Cdc37
Cdc37
PP5-His6
D
In vitro
– Hsp90α
– CK1δ
+ CK1δ
Time (min) 0 10 20 30 0 10 20 30
Phos-S13-Cdc37
Cdc37
PP5-His6
E
In vitro
ATP – +
CK1δ-GST
Co-IP
Phos-Thr
PP5-His6
IP
F
In vitro
+ CK1δ
– ATP
+ ATP
Time (min) 0 10 20 30 0 10 20 30
Phos-S13-Cdc37
Cdc37
PP5-His6
G
HEK293
EV
WT-PP5
T362A
T362E
Phos-S211-GR
SE
LE
GR
Phos-S13-Cdc37
Cdc37
PP5-FLAG
GAPDH
H
HEK293
IP: FLAG
EV
WT-PP5
T362A
T362E
GR
Co-IP
Input
Cdc37
Co-IP
Input
Hsp90
Co-IP
Input
PP5-FLAG
IP

**Figure 8. CK1δ mediated phosphorylation of PP5 activates and increases the rate of phosphatase activity.**

**(A**) Dephosphorylation of phospho-S13-Cdc37 with a recombinant wild-type PP5-$His_6$ and phosphomimetic T362E-PP5-$His_6$, in the presence of Hsp90α. Rate of Cdc37 dephosphorylation was assessed by immunoblotting with a phospho-specific S13-Cdc37 antibody over time (minutes).
**(B)** Recombinant wild-type PP5-$His_6$ was phosphorylated by CK1δ *in vitro* and then used in the dephosphorylation of phospho-S13-Cdc37 *in vitro*. The assay was performed in presence of Hsp90α. PP5 activity was assessed with immunoblotting using a phospho-specific S13-Cdc37 antibody over time (minutes). *Legend continues on next page.*
**(C)** Dephosphorylation of phospho-S13-Cdc37 withrecombinant wild-type PP5-$His_6$ and phosphomimetic T362E-PP5-$His_6$ was performed in the absence of Hsp90α. Activity was assessed with immunoblotting using a phospho-specific S13-Cdc37 antibody over time (minutes).
**(D)** Recombinant wild-type PP5-$His_6$ was phosphorylated by CK1δ *in vitro* and then used in the dephosphorylation of phospho-S13-Cdc37 *in vitro* without Hsp90α. PP5 activity was assessed with immunoblotting using a phospho-specific S13-Cdc37 antibody over time (minutes).
**(E)** Recombinant PP5-His6 was used in an in vitro kinase assay with CK1δ-GST. PP5-His6 was immunoprecipitated (Vaughan et al.) and threonine phosphorylation of PP5 as well as co-immunoprecipitation (Co-IP) of CK1δ-GST were examined by immunoblotting with anti-phosphothreonine and anti-GST antibodies.
**(F)** Recombinant wild-type PP5-His6 was phosphorylated by CK1δ in vitro in the presence (+) or absence (–) of ATP. PP5-His6 proteins were then used in the dephosphorylation of phospho-S13-Cdc37 in vitro without Hsp90α. PP5 activity was assessed with immunoblotting using a phospho-specific S13-Cdc37 antibody over time (minutes).
**(G)** PP5-FLAG and T362-PP5 phosphomutants (T362A and T362E) were transiently transfected in HEK293 cells. Cdc37, phospho-S13-Cdc37, GR and phospho S211-GR protein levels were examined by immunoblotting. Empty vector (EV) was used as a control, GAPDH was used a loading control.
**(H)** Wild-type PP5-FLAG, non-phosphorylating T362A-PP5-FLAG and the phosphomimetic T362E-PP5-FLAG were transiently expressed and IP from HEK293 cells. Co-IP of GR, Cdc37 and Hsp90 were examined by immunoblotting. Results presented in this figure were obtained by Dr. Mehdi Mollapour and former graduate student Diana Dunn.

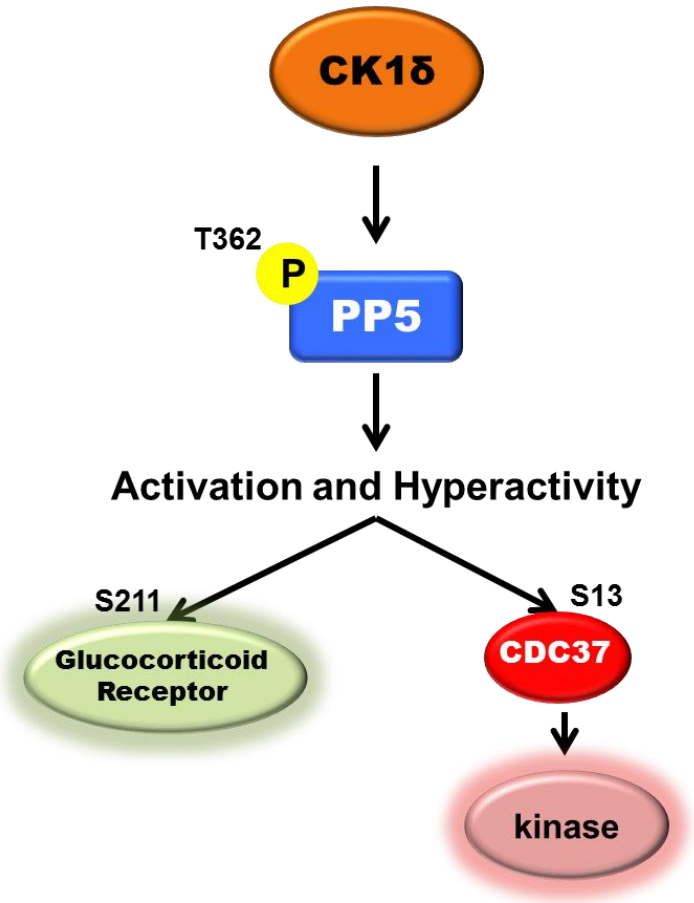


**Figure 9. CK1δ phosphorylates PP5 leading to PP5 activation and hyperactivity.**

CK1δ phosphorylates PP5 at T362, which results in the activation and hyperactivity of PP5 toward its *bona fide* substrates glucocorticoid receptor (GR) and Cdc37.

### 2.2.3 VHL E3 ligase targets PP5 independent of hypoxia

To determine the binding partners of the PP5 that may be involved in its regulation, we immunoprecipitated the endogenous PP5 from HEK293 cells and identified its intracellular binding proteins by mass spectrometry (MS) analysis (described in Chapter 3-Materials and Methods). Our interactome data identified the tumor suppressor Von Hippel-Lindau (VHL) as a binding partner of PP5 (Table 2). VHL forms a multi-protein complex VCB-Cul2 (VHL-Elongin C-Elongin B-Cullin-2) and Rbx1 that acts as a ubiquitin-ligase

(E3) (Gossage et al., 2015; Kamura et al., 1999; Stebbins et al., 1999) and directs proteasome-dependent degradation of targeted proteins such as hypoxia-inducible factors (HIF1α or HIF2α) (Kamura et al., 2000). *VHL* is expressed as two known isoforms; $VHL_{30}$, with an apparent molecular weight of ~24 to 30 kDa ($VHL_{30}$), and $VHL_{19}$, roughly 19 kDa in size (Iliopoulos et al., 1995). Both isoforms appear to retain tumor suppressor activity, however $VHL_{30}$ is the commonly examined isoform. Here, we confirmed our interactome data by immunoprecipitating endogenous PP5 from HEK293 cells and detecting $VHL_{30}$ (Figure 10A).

The reciprocal immunoprecipitation of the endogenous $VHL_{30}$ yielded PP5 (Figure 10B). Since VHL is the substrate recognition subunit of an E3 ubiquitin ligase, we overexpressed $VHL_{30}$ in the VHL deficient clear cell renal cell carcinoma (ccRCC) cell line, 786-O, and observed down-regulation of endogenous PP5 by immunoblotting (Figure 10C). We next transiently transfected and expressed PP5-FLAG in the 786-O cell line. Using immunoprecipitation and immunoblotting, we were unable to detect PP5 ubiquitination in these cells (Figure 10D), even when treated with 50 nM proteasome inhibitor bortezomib (BZ) for 2 hr (Figure 10D). However, transient co-expression of PP5-FLAG and $VHL_{30}$-$His_6$ in 786-O cells for 16 hr and subsequent treatment with 50 nM BZ for 2 hr led to detection of distinct ubiquitination bands, suggesting multi-monoubiquitination of PP5-FLAG (Figure 10D). It is noteworthy that anti-ubiquitin antibody (P4D1) used in these experiments recognizes both mono and polyubiquitination. Taken together, these data suggest that VHL E3 ligase ubiquitinates and degrades PP5 in the proteasome.

**Table 2. Cellular proteins associated with PP5 identified by mass spectrometry.**

VHL (highlighted in yellow) was found to interact with PP5. This interaction was the only one further investigated due to the role of VHL as a tumor suppressor and the role VHL mutations play in kidney cancer. Mass spectrometry data obtained by our collaborator Dr. Timothy A. Haystead.

| Protein | MW | Protein Score | Protein Score C.I.% | Total Ion Score | Total Ion C.I. % | Peptides | Accession Number |
|---|---|---|---|---|---|---|---|
| Serine/threonine-protein phosphatase 5-PP5 | 56842.2 | 95 | 100 | 80 | 100 | FYSQAIELNPSNAIYYGN<br>TECYGYALGDATR<br>AFLEENNLDYIIR<br>AEGYEVAHGGR<br>AASNMALGKFR<br>TQANDYFK | gi\|324021715 |
| Actin, cytoplasmic 2 -ACTG1 | 41765.8 | 351 | 100 | 303 | 100 | TTGIVMDSGDGVTHTVPIYEGYALPHAILR<br>KDLYANTVLSGGTTMYGPADR<br>DLYANTVLSGGTTMYPGADR<br>VAPEEHPVLLTEAPLNPK<br>SYELPDGQVITIGNER<br>QEYDESGPSIVHR<br>AVFPSIVGRPR<br>AGFAGDDAPR<br>GYSFTTTAER<br>DLTDYLMK | gi\|823672677 |
| Vimentin | 53619.1 | 49 | 72 | 29 | 98 | VEVERDNLAEDIMRLREK<br>STRSVSSSSYRRMFGGP<br>SLYASSPGGVYATR<br>ISLPLPNFSSLNLR<br>LGDLYEEEMR<br>QDVDNASLAR<br>GTASRPSSSR | gi\|340218 |
| Actin, cytoplasmic 1 -ACTB | 41709.7 | 77 | 100 | 50 | 100 | MDDDIAALVVDNGSGMC<br>MTQIMFETFNTPAMYVAI<br>VAPEEHPVLLTEAPLNPK<br>SYELPDGQVITIGNER<br>QAVLSLYASGR<br>AGFAGDDAPR<br>GYSFTTTAER<br>DLTDYLMK | gi\|823671251 |
| Von Hippel-Lindau disease tumor suppressor | 24137.9 | 5 | 5 | 42 | 94 | HGIADLFR | gi\|319655736 |

Finally, we examined PP5 protein levels in Caki-1 cells cultured in normoxia and hypoxia (1%$O_2$, 5%$CO_2$, 94%$N_2$). While HIF1α levels increased under hypoxia, PP5 levels were similar to normoxia (Figure 10E). Finally, previous work has indicated that transcription of PP5 can be mediated by HIF1 (Zhou et al., 2004). We examined this possibility by using small interfering RNA (siRNA) to silence *HIF1α* or *HIF2α* in HEK293 cells. Our results showed that neither HIF1α nor HIF2α are involved in regulation of PP5 (Figure 10F). We conducted a similar experiment in 786-O ccRCC cells and silenced only

*HIF2α* (HIF1α is down-regulated in these cells). These data indicate that VHL ubiquitinates PP5 independent of hypoxia.

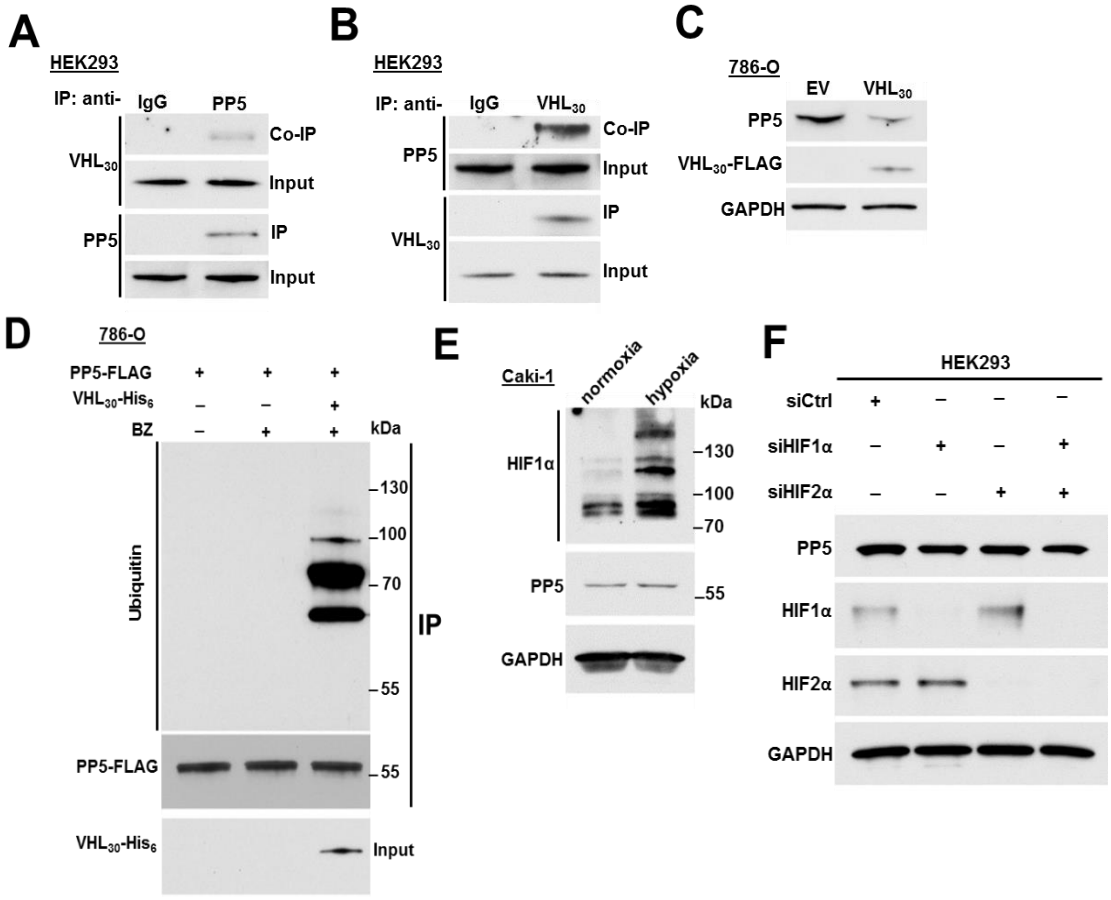


**Figure 10. VHL E3 ligase ubiquitinates PP5 independent of hypoxia.**

**(A**) Endogenous PP5 was immunoprecipitated (Vaughan et al.) from HEK293 cells and co-immunoprecipitation (Co-IP) of $VHL_{30}$ was assessed by immunoblotting.
**(B)** Endogenous $VHL_{30}$ was IP from HEK293 cells and Co-IP of PP5 was examined by immunoblotting.
**(C)** $VHL_{30}$-FLAG or empty vector (EV) was transiently over-expressed in 786-O cells and endogenous PP5 protein levels were assessed by immunoblotting. GAPDH was used a loading control.
**(D)** 786-O cells transiently expressing PP5-FLAG, were treated with or without 50 nM proteasome inhibitor bortezomib (BZ) for 2 hr. PP5-FLAG was also co-expressed with $VHL_{30}$-$His_6$ with additional treatment of 50 nM BZ for 2 hr. PP5-FLAG was IP and its ubiquitination was assessed by immunoblotting.
**(E)** Caki-1 cells cultured in normoxia and hypoxia (1%$O_2$, 5%$CO_2$, 94%$N_2$). PP5 and HIF1α protein levels were examined by immunoblotting using anti-PP5 and anti-HIF1α antibodies. GAPDH was used a loading control.
**(F)** *HIF1α* or *HIF2α* were silenced by small interfering RNA (siRNA) in HEK293 cells. HIF1α, HIF2α and PP5 protein levels were examined by immunoblotting using anti-HIF1α, anti-HIF2α and anti-PP5 antibodies. GAPDH was used a loading control. Results presented in this figure were obtained by former lab member Diana Dunn.

### 2.2.4 VHL ubiquitinates K185/K199-PP5

Based on the data available on PhosphoSitePlus® (www.phosphosite.org), which is an online systems biology resource providing comprehensive information on PTMs of human proteins, we identified five ubiquitinated lysine sites (K32, K40, K185, K199 and K320) on PP5 (Figure 11A). These sites are all located on the surface of the PP5 protein. We individually mutated these lysine sites to a non-ubiquitinating arginine residue and transiently expressed them in HEK293 cells (Figure 11B). Ubiquitination of the wild-type PP5 was detectable by immunoprecipitation and immunoblotting techniques (Figure 11B). However, ubiquitination of PP5 was significantly reduced in the K185R and K199R mutants (Figure 11B).

We next created a K185R/K199R-PP5-FLAG double mutant and transiently expressed it in HEK293 cells. Ubiquitination of this mutant was undetectable by immunoprecipitation and immunoblotting experiments (Figure 11C). To determine if VHL is responsible for ubiquitination of these sites, we used an *in vitro* ubiquitination assay kit (Millipore) with the VCB-Cul2 ($VHL_{30}$-Elongin C-Elongin B-Cullin-2) complex. As mentioned earlier, VHL is part of a multi-protein complex, VCB-Cul2 and Rbx1, acting as an ubiquitin-ligase (E3) and directing proteasome dependent degradation of targeted proteins. Next, bacterially expressed and purified wild-type PP5-$His_6$ and K185R/K199R-PP5-$His_6$ double mutant were used in our *in vitro* ubiquitination assay.

Our data show that the recombinant wild-type PP5-$His_6$ but not the K185R/K199R-PP5-$His_6$ mutant were subject to ubiquitination. Based on the immunoblots and the appearance of the bands, our data suggest that PP5 is subject to multi-monoubiquitination (Figure 11D), therefore suggesting that VHL targets K185/K199-PP5 for ubiquitination. To gain further evidence of VHL-mediated ubiquitination of K185/K199-PP5 in cells, we

transiently co-expressed the wild-type PP5-FLAG or K185R/K199R-PP5-FLAG with $VHL_{30}$-$His_6$ for 16 hr in VHL-null 786-O cells, then treated them with 50nM BZ for 2 hr. We were only able to detect the ubiquitination of the wild-type PP5 but not the K185R/K199R-PP5 double mutant (Figure 11E). The K185R-, K199R-PP5 single or double mutants interacted with the same affinity as the wild-type PP5 to $VHL_{30}$ (Figure 11F). Therefore, the reduced ubiquitination of these mutants could not be due to their inability to bind to $VHL_{30}$. Taken together, our data show that VHL E3 ligase ubiquitinates K185 and K199 residues in PP5.

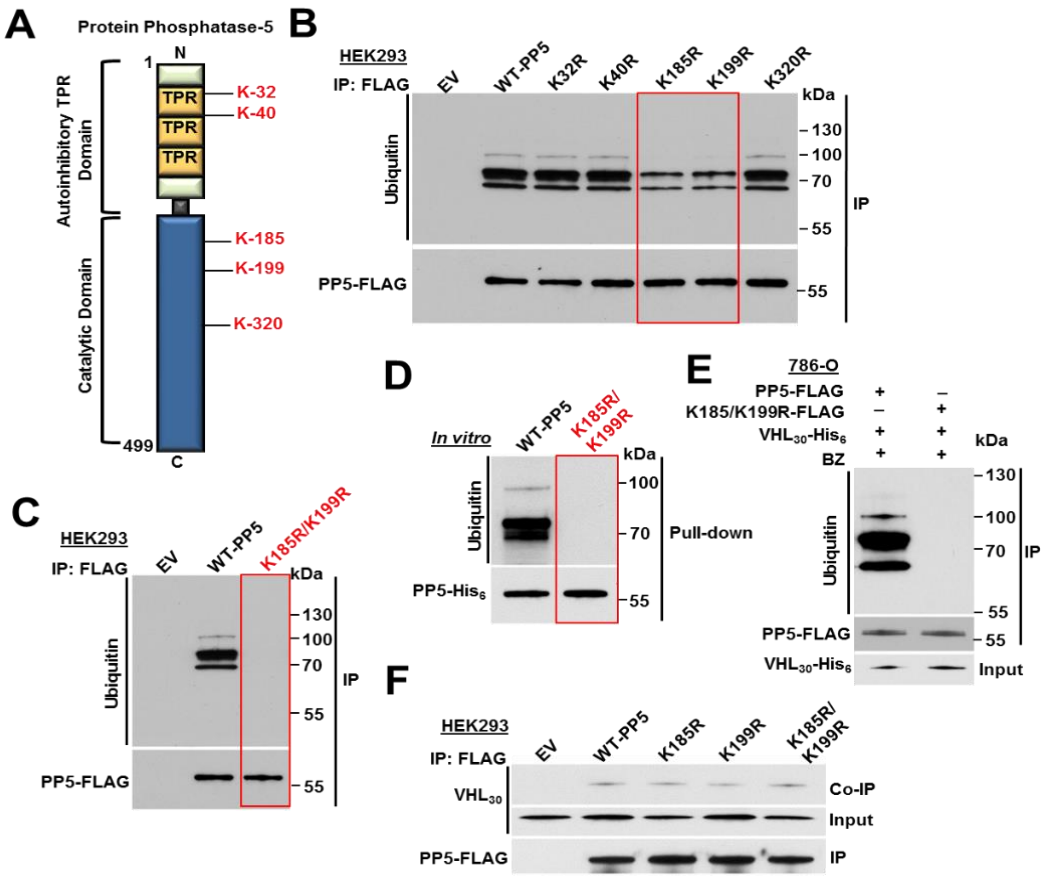


**Figure 11. VHL-mediated ubiquitination and proteasomal degradation of K185/K199-PP5.**

**(A**) Schematic representation of PP5 with highlighted lysine residues possibly subject to VHL mediated ubiquitination.
**(B)** Wild-type PP5-FLAG and its potentially non-ubiquitinating lysine mutants were transiently expressed and immunoprecipitated (Vaughan et al.) from HEK293 cells. Ubiquitination of PP5 was examined by immunoblotting. Empty vector (EV) was used as a control.
**(C)** Wild-type PP5-FLAG and its non-ubiquitinating K185/K199R mutant were transiently expressed and IP from HEK293 cells. Ubiquitination of PP5 was examined by immunoblotting anti-ubiquitin antibody. Empty vector (EV) was used as a control.
**(D)** Recombinant PP5-$His_6$ and K185/K199R double mutant were used in an *in vitro* ubiquitination assay with VCB-Cul2 ($VHL_{30}$-Elongin C-Elongin B-Cullin-2) and Rbx1, which acts as an ubiquitin-ligase (E3). Ubiquitination of PP5 was assessed with immunoblotting.
**(E)** PP5-FLAG or K185/K199R-PP5-FLAG double mutant were co-transfected with $VHL_{30}$-$His_6$ in 786-O cells and then after 24 hr treated with 50 nM BZ for 2 hr. PP5-FLAG or K185/K199R-PP5-FLAG was IP and ubiquitination was assessed by immunoblotting.
**(F)** PP5-FLAG, K185-PP5-FLAG, K199R-PP5-FLAG, K185/K199R-PP5-FLAG and empty vector (EV) were individually and transiently expressed in HEK293 cells. They were IP and their interactions with $VHL_{30}$ were assessed in the Co-IP by immunoblotting. Results presented in this figure were obtained by former lab member Diana Dunn.

### 2.2.5 PP5 down-regulation causes apoptosis in VHL null ccRCC cells

To gain further insight into the significance of PP5 stability and hyperactivity in ccRCC, I first examined PP5 protein levels in tumors and adjacent normal tissues from nine patients with ccRCC. Within 10 min of removal of tumors by radical or partial nephrectomy, tumors and adjacent normal tissues were dissected into 10 $mm^3$ pieces followed by staining with haematoxylin and eosin (H&E) (Figure 12A) or protein extraction (Figure 12B). Our data showed that $VHL_{30}$ is absent in the ccRCC tumors. Conversely, PP5 and CK1δ were both upregulated in the tumors compared to the adjacent normal tissues (Figure 12B). This indicates that, unlike in normal cells where VHL ubiquitinates PP5 signaling for its degradation, in VHL-null ccRCC cells PP5 accumulates, likely resulting in the upregulation of downstream angiogenic factors (Figure 13).

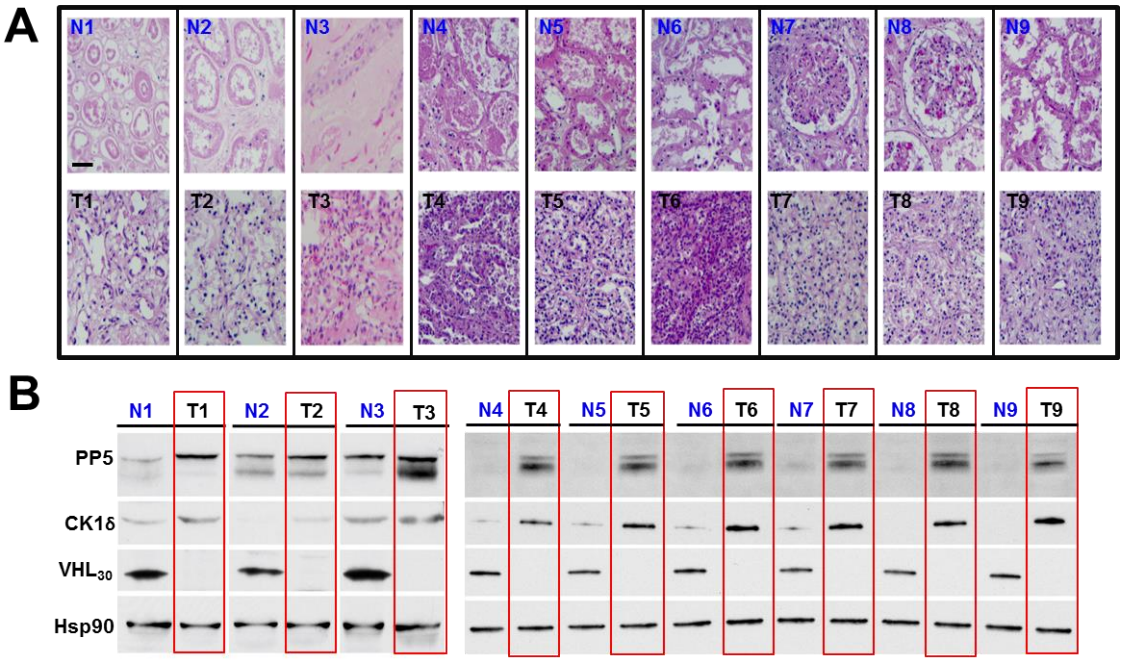


**Figure 12. PP5 is upregulated in VHL-null ccRCC patient tumor samples.**

**(A)** Clear cell renal cell carcinoma (ccRCC) tumors, (T) and adjacent normal tissues (N) were stained with haematoxylin and eosin (H&E). Bar scale represents 200μm.
**(B)** Proteins were extracted from above tumors and adjacent normal tissues and expression of PP5, CK1δ, $VHL_{30}$ and Hsp90 was examined by immunoblotting. Hsp90 was used a loading control.

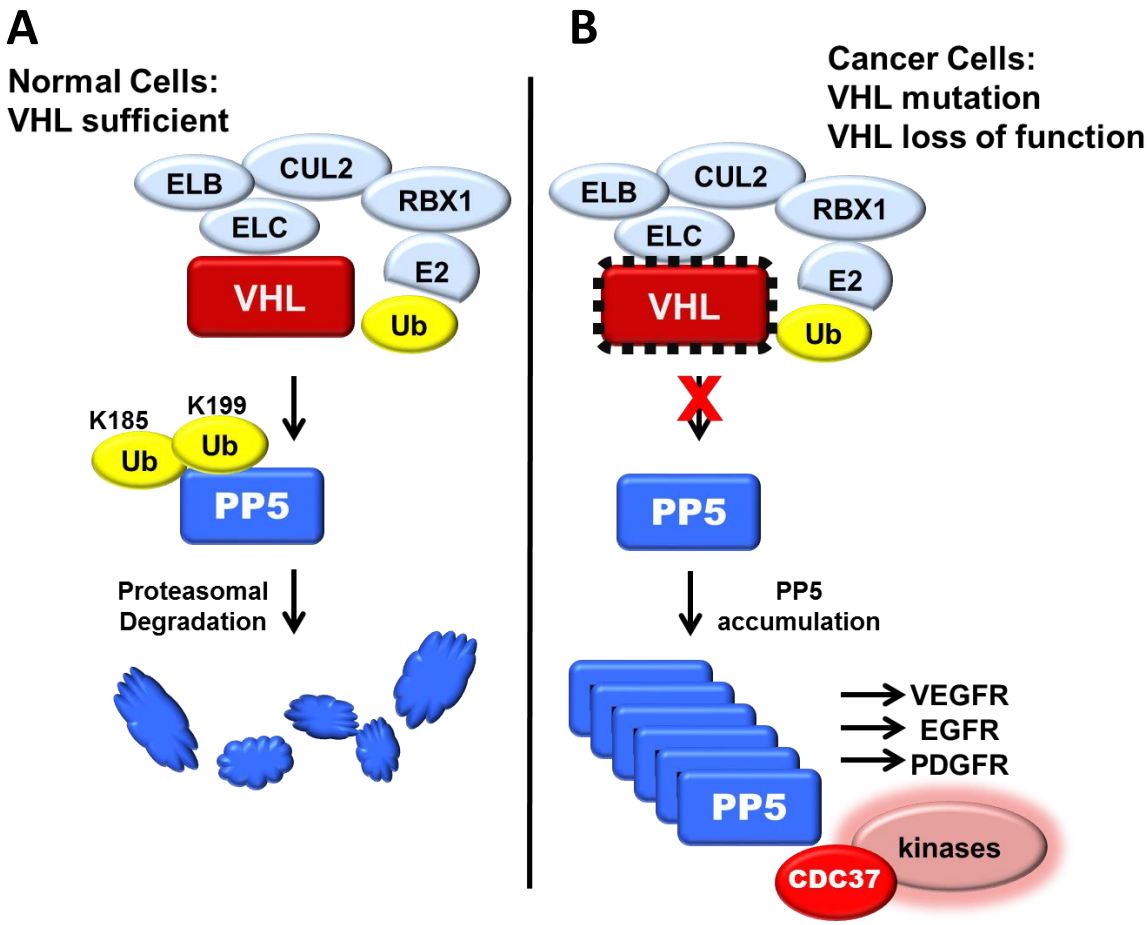


**Figure 13. VHL regulation of PP5 in normal and VHL-null cancer cells.**

**(A)** In normal cells, under normoxic conditions, VHL ubiquitinates PP5 at K185 and K199 leading to the proteasomal degradation of PP5.
**(B)** In ccRCC cancer cells when VHL is mutated, it is unable to recognize and ubiquitinate PP5, which leads to PP5 accumulation and increase of PP5 activity towards its substrates Cdc37 and GR.

We confirmed this data by using established *VHL*-deficient (786-O and A498) and *VHL*-containing (Caki-1) ccRCC cell lines. Our data showed that PP5 was upregulated in the 786-O and A498 cell lines compared to Caki-1 cells, and that CK1δ levels displayed a similar expression pattern (Figure 14A). This pattern was consistent with dephosphorylation of PP5 substrates, Cdc37 and GR. These were both more dephosphorylated in 786-O and A498 cells compared to the VHL-containing Caki-1 cells

(Figure 14A). We next used siRNA to silence *PP5* in 786-O and Caki-1 cells and observed induction of the pro-apoptotic markers cleaved caspase-3 and cleaved-poly-ADP-ribose polymerase (PARP) only in the VHL-null 786-O cells (Figure 14B). Furthermore, siRNA silencing of *PP5* in A498 cells (VHL-null cell line) also led to induction of the apoptotic markers cleaved caspase-3 and cleaved-PARP (Figure 14C).

To evaluate the threonine phosphorylation status of PP5 in the VHL-null cells, we immunoprecipitated the endogenous PP5 from 786-O and Caki-1 cells and showed that PP5 from VHL-null 786-O cells was hyperphosphorylated on threonine residues (Figure 14D). Because IC261 is a potent specific inhibitor of CK1δ/ε, we next examined whether pharmacologic inhibition of CK1δ, reduces threonine phosphorylation of PP5. 786-O cells treated or untreated with 2 μM IC261 16 hr and PP5 was immunoprecipitated and as expected, IC261 treatment led to a marked reduction of PP5 threonine phosphorylation but not serine phosphorylation (Figure 14E). Taken together, our data show that PP5 is upregulated, and also phosphorylated by CK1δ in VHL-null ccRCC cells. Consequently, downregulation of *PP5* in VHL-null cells causes apoptosis.

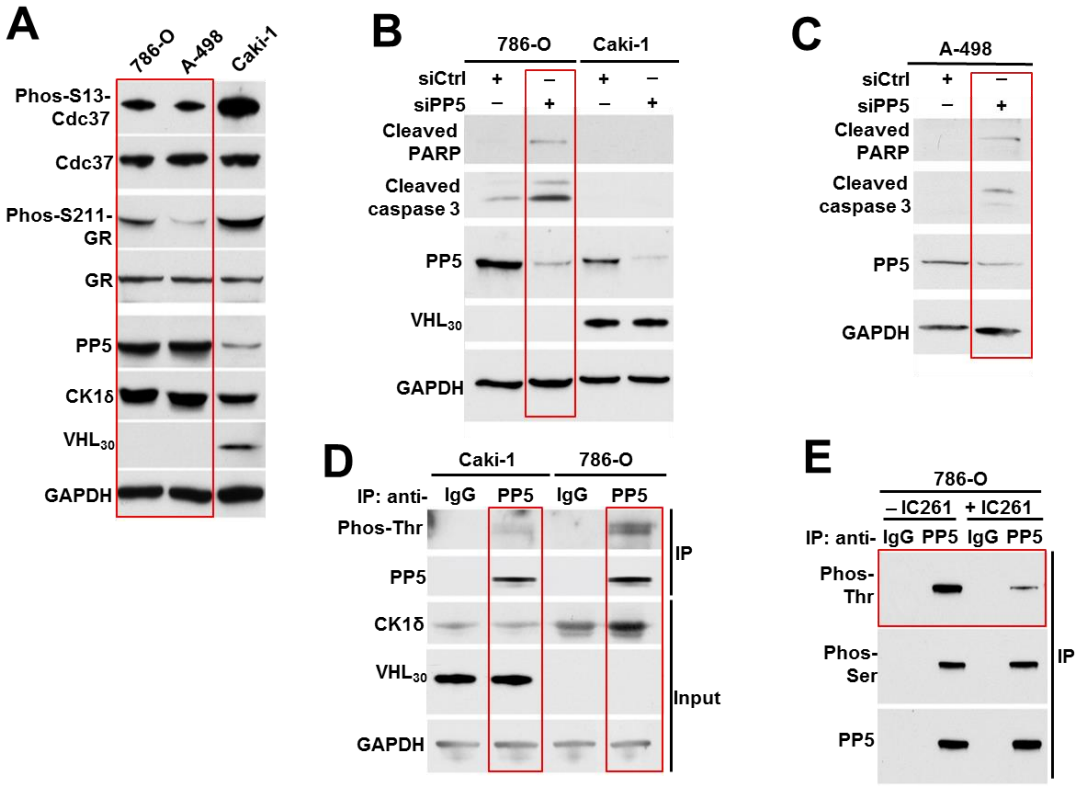


**Figure 14. Downregulation of PP5 induces apoptosis in VHL deficient ccRCC cells.**

**(A**) PP5, Cdc37 and phosphorylated S13-Cdc37, GR and phosphorylated S211-GR, CK1δ and $VHL_{30}$ proteins from ccRCC cell lines 786-O, A498 (VHL-deficient) and Caki-1 (VHL-containing) were assessed by immunoblotting. GAPDH was used as a loading control.
**(B)** *PP5* was silenced by siRNA in 786-O and Caki-1 cells. siCtrl represents the non-targeting siRNA control. Induction of apoptotic markers shown by immunoblotting using anti-cleaved caspase-3 and cleaved-PARP antibodies. GAPDH was used a loading control.
**(C)** Targeted siRNA was used to silence *PP5* in A498 cells. siCtrl represents the non-targeting siRNA control. Induction of apoptotic markers shown by immunoblotting using anti-cleaved caspase-3 and cleaved-PARP antibodies. PP5 protein levels were also examined by immunoblotting. GAPDH was used as a control.
**(D)** PP5 was immunoprecipitated (Vaughan et al.) from ccRCC cell lines, Caki-1 and 786-O, lysates using anti-PP5 antibody or IgG (control). Threonine phosphorylation of PP5 was assessed by immunoblotting with anti-phosphothreonine antibody. GAPDH was used a loading control.
**(E)** PP5 was isolated from the lysates of 786-O cell treated with 2 µM IC261 for 16 hr using anti-PP5 or IgG (control) antibodies. Threonine phosphorylation of PP5 was examined by immunoblotting using anti-phosphothreonine antibody. Anti-phosphoserine antibody was used as a control.
Experimental data presented in this figure was obtained by Mark Woodford, and former graduate student Diana Dunn.

### 2.2.6 PP5 upregulation provides a pro-survival mechanism in VHL null ccRCC cells

I next examined whether pharmacologic inhibition of CK1δ, causing apoptosis in VHL-null cells; A498 and 786-O. I used Caki-1 cells as a control since this ccRCC cell line has the *VHL* gene. These cell lines were treated with different amounts of IC261, which is a potent specific inhibitor of CK1δ/ε. Increasing amounts of IC261 correlated with increased induction of the pro-apoptotic markers cleaved caspase-3 and cleaved-PARP only in A498 and 786-O (VHL-null) cells (Figure 15).

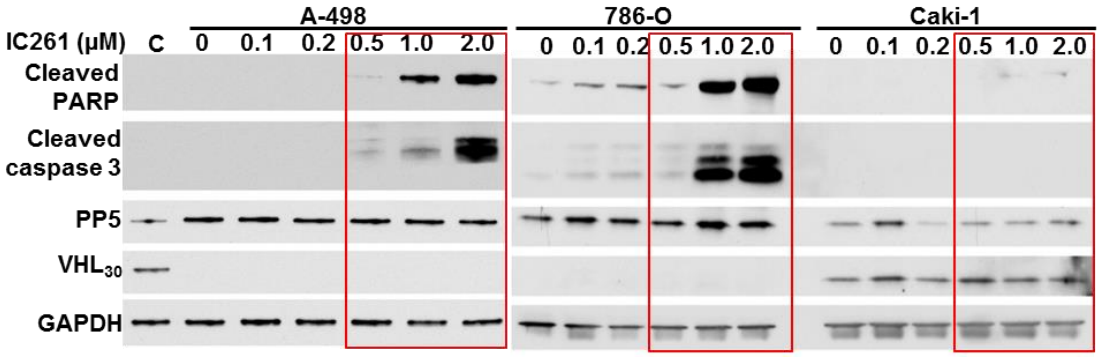


**Figure 15. CK1δ inhibition induces apoptosis in VHL-null ccRCC cells.**

ccRCC cell lines A498, 786-O and Caki-1 were treated with indicated amounts of CK1δ inhibitor IC261 for 16 hr and induction of apoptotic markers shown by immunoblotting using anti-cleaved caspase-3 and cleaved-PARP antibodies. GAPDH was used a loading control.

Another hallmark of apoptosis is the loss of cell membrane integrity, which can be monitored by annexin V/propidium iodide (AV/PI) staining. A498, 786-O and Caki-1 cells were treated with 0.5μM and 2.0μM IC261 for 16 hr prior to analysis of apoptosis by AV/PI staining. Treatment of the A498 and 786-O cells with 2.0μM IC261 resulted in cells progressing through the AV+/PI– apoptotic quadrant (Figure 16A). However, this effect was not observed in Caki-1 cells following the same treatment with IC261 (Figure 16A). I next examined the effects of IC261 on proliferation of ccRCC cell lines. A498, 786-O and Caki-1 cells were treated with different amounts of CK1δ inhibitor, IC261. After 72 hours,

proliferation was measured by the 3-(4, 5-dimethylthiazolyl-2)-2, 5-diphenyltetrazolium bromide (MTT) assay. The data revealed that 2.0µM IC261 significantly inhibited the proliferation of A498 and 786-O cells compared to Caki-1 cells (Figure 16B). A hallmark

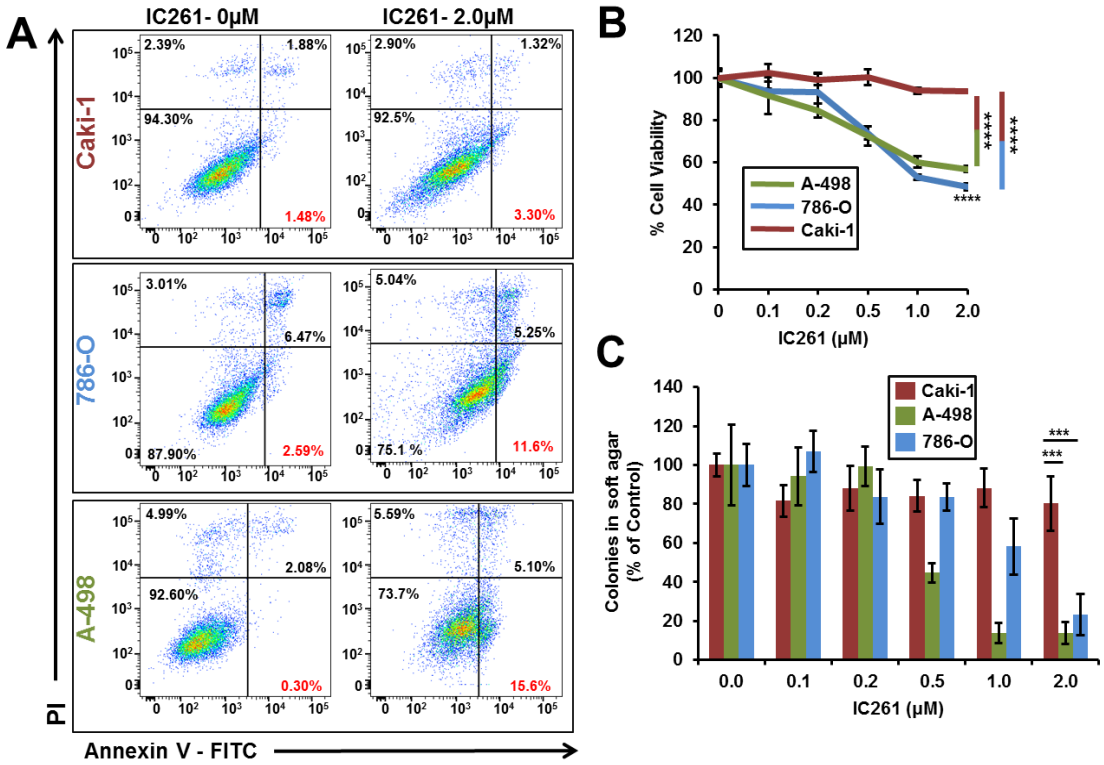


**Figure 16. CK1δ inhibition decreases proliferation in VHL-null ccRCC cells.**

**(A)** AV/PI graphs of Caki-1, A498 and 786-O cells untreated (0µM) or treated with 2µM IC261 for 16hr for 2 hr. The top left quadrants represent dead cells stained only with PI. The bottom right quadrants represent apoptotic cells stained only with AV. The top right quadrants represent cells stained with both PI and AV (secondary necrosis and late apoptosis). Percentage of each stained cell population is indicated. Dot plots shown are representative of one of three independent experiments.
**(B)** MTT assay of A498, 786-O and Caki-1 cells treated with indicated amounts of IC261. The errors bars represent the SD of three independent experiments (****$p < 0.0001$).
**(C)** Anchorage-independent growth of A498, 786-O and Caki-1 cells treated with indicated amounts of IC261 in soft agar. Colony number was quantified. The errors bars represent the SD of three independent experiments (***$p < 0.0005$).

of tumorigenic cells is their anchorage-independent growth property, which is measurable by soft agar assay. Treating the A498 and 786-O cells with 2.0µM IC261 significantly reduced the anchorage-independent growth of these cells compared to the Caki-1 cell line (Figure 16C).

Although treatment of VHL-null cells with IC261 caused apoptosis, it is unclear if this effect was due to lack of PP5 phosphorylation and activity. To address this question, wild-type PP5-FLAG and its phospho-PP5 mutants T362A and T362E were transiently expressed in 786-O cells. Treating the cells expressing empty vector (EV) or the non-phosphorylatable T362A-PP5-FLAG mutant with 2.0μM IC261 led to induction of the pro-apoptotic markers cleaved caspase-3 and cleaved-PARP. This effect was significantly reduced upon expression of the wild-type PP5-FLAG and completely abrogated with the phosphomimetic T362E-PP5-FLAG mutant (Figure 17A). This data was further confirmed by using the MTT assay. The data showed that treating the 786-O cells transiently expressing EV or non-phosphorylatable T362A-PP5-FLAG mutant with 2.0μM IC261 caused a marked reduction in cell proliferation, whereas this effect was not observed in 786-O cells expressing wild-type PP5-FLAG and phospho-mutant T362E-PP5 (Figure

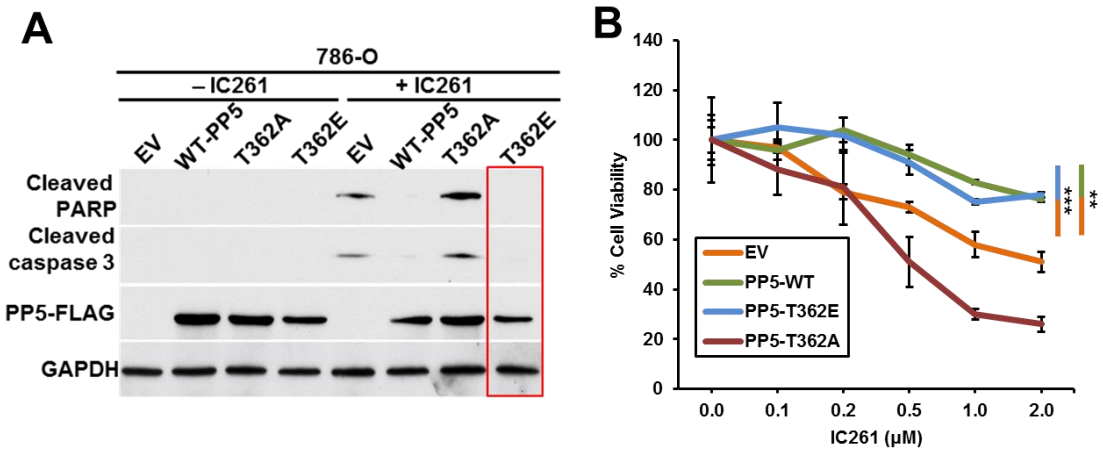


**Figure 17. Overexpression of PP5-T362E phosphomimetic protects VHL-null ccRCC cells from CK1δ inhibition induced apoptosis.**

**(A**) Wild-type PP5-FLAG, non-phosphorylating T362A-PP5-FLAG and the phosphomimetic T362E-PP5-FLAG were transiently expressed in 786-O cells. Cells were then either untreated (-IC261) or treated (+IC261) with 2 μM IC261 for 16 hr and induction of apoptotic markers shown by immunoblotting using anti-cleaved caspase-3 and cleaved-PARP antibodies. GAPDH was used a loading control.
**(B)** MTT assay of 786-O cells transiently expressing wild-type PP5-FLAG, T362A-PP5-FLAG and T362E-PP5-FLAG and then treated with indicated amounts of IC261. The errors bars represent the SD of three independent experiments (**p < 0.005 and ***p < 0.0005).

17B). Taken together, our data shows that pharmacologic inhibition of CK1δ causes apoptosis in ccRCC cells, and this effect is through lack of threonine phosphorylation of PP5 and reduced phosphatase activity.

### 2.2.7 PP5 inhibition leads to apoptosis through the extrinsic pathway

Having established that PP5 plays a pro-survival role in VHL-*null* ccRCC cancers, I sought to determine which apoptotic pathway was activated with PP5 inhibition. PP5 expression was knocked down in 786-O and A498 cells with siPP5, and levels of apoptotic markers were observed. Both 786-O and A498 cells showed an increase in, not only, general apoptotic markers cleaved PARP and cleaved caspase 3, but a dramatic increase in cleaved caspase 8 (Figure 18). Meanwhile, caspase 9 levels were unaffected in both cell lines. The increase in cleaved caspase 8 is indicative of the induction of the extrinsic apoptotic pathway.

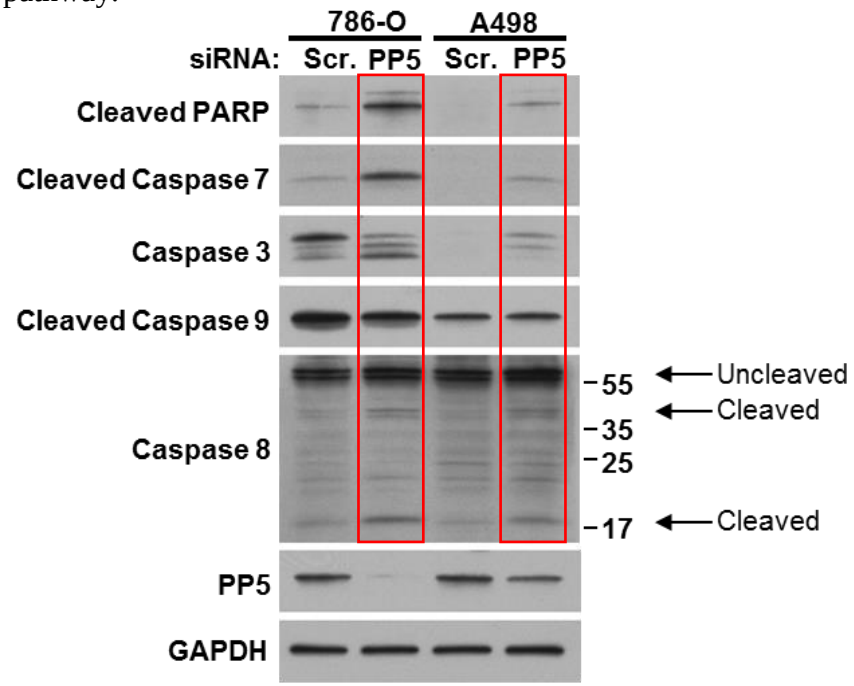


**Figure 18. PP5 knockdown causes induction of the extrinsic pathway.**

VHL-*null* ccRCC 786-O and A498 cells were treated with scrambled (scr.) or PP5-targeting siRNA. PP5 levels shown by immunoblotting with anti-PP5 antibody. Induction of apoptotic markers shown by immunoblotting using anti-cleaved caspase-3, cleaved-PARP, cleaved-caspase 7, cleaved-caspase 9, and caspase 8 antibodies. GAPDH was used a loading control.

This conclusion was confirmed when I treated 786-O cells with IC261 for 16 hr and observed the expression levels of apoptotic markers. As with the siPP5 treatment, 786-O cells treated with IC261 showed a strong concentration-dependent increase in cleaved-PARP, and cleaved caspases 3 and 8. And as before, caspase 9 remained inactive with unchanged levels (Figure 19A). As expected, the addition of 10μM pan-caspase inhibitor z-VAD-fmk abrogated the induction of apoptosis (Figure 19B). These data show that both knockdown of PP5 expression and the decrease of PP5 activity both lead to the induction of apoptosis through the extrinsic pathway (Figure 20).

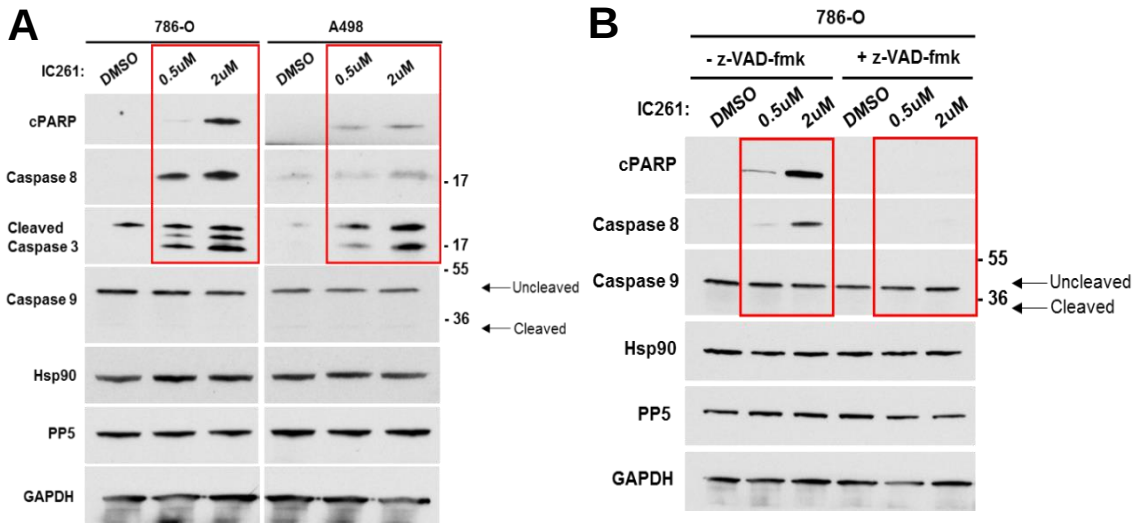


**Figure 19. Inhibition of PP5 with IC261 causes induction of the extrinsic pathway.**

**(A)** VHL-*null* ccRCC cells (786-O and A498) were treated with indicated amounts of IC261 for 16 hr. Results show that PP5 inhibition leads to apoptosis through the induction of the extrinsic pathway. Induction of apoptotic markers shown by immunoblotting using anti-cleaved caspase-3, cleaved-PARP, cleaved-caspase 9, and caspase 8 antibodies. GAPDH was used a loading control.
**(B)** 786-Os were treated with 10μM pan-caspase inhibitor, z-VAD-fmk, for 1 hour prior to the addition of indicated amounts of IC261. Cells were incubated for 16 hr post IC261 treatment. Induction of apoptotic markers shown by immunoblotting using anti-cleaved-PARP, cleaved-caspase 9, and caspase 8 antibodies. GAPDH was used a loading control.

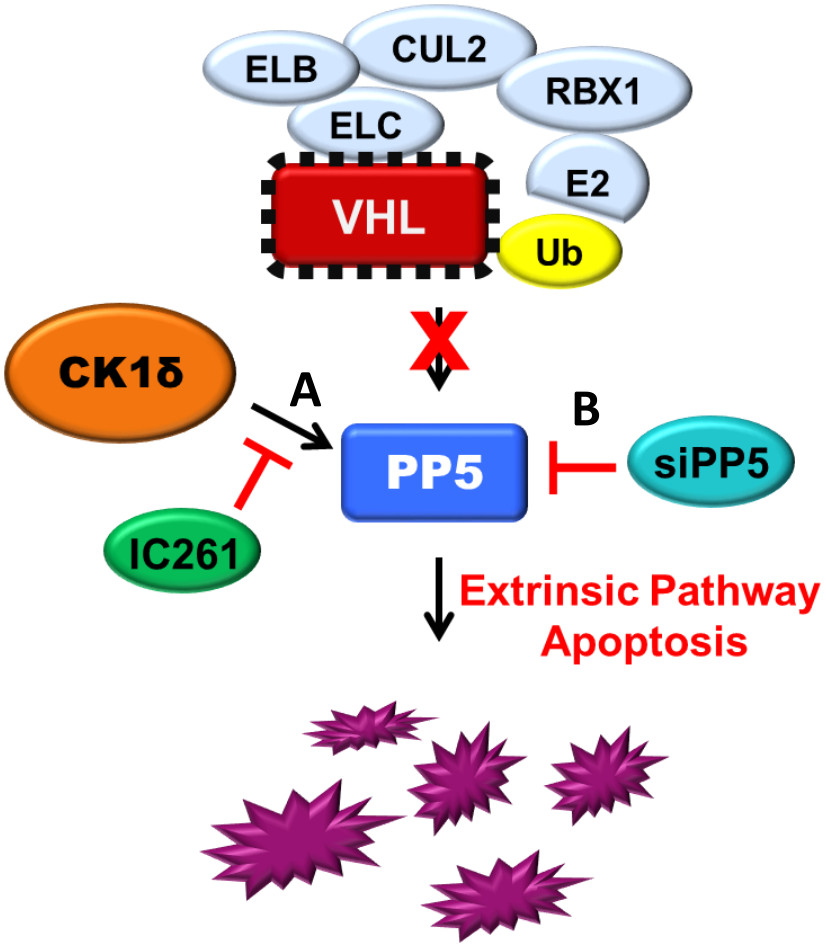


**Figure 20. Inhibition of PP5 activity causes induction of the extrinsic pathway.**

**(A)** Inhibition of CK1δ with small molecule inhibitor IC261 prevents PP5 activation and leads to cancer cell apoptosis through the extrinsic pathway.
**(B)** Down regulation of PP5 expression with siRNA leads to the activation of the extrinsic apoptotic pathway.

## 2.9 Discussion

PP5 is a crucial phosphatase that is responsible for regulating cellular stress response, cell signaling, proliferation, DNA damage, and even cell death (Golden et al., 2008b). Although PP5 activity has been most thoroughly studied in complex with Hsp90, previous data within our lab showed that PP5 can also act independently of Hsp90. PP5 undergoes post translational modifications (PTMs), and is itself phosphorylated at T362 by CK1δ (Figures 5 and 6). This phosphorylation acts as an "on switch" and increases PP5 activity, making it hyperactive towards *bona fide* substrates such as Cdc37 and GR (Figure 21). But more importantly, these novel findings show that PP5 phosphorylated at T362 can dephosphorylate its substrates in a manner completely independent of Hsp90 (Figure 8).

Until recently, PP5 was thought to only have a low basal activity unless it was directly activated by Hsp90 or other known activators such as arachidonic acid (Yang et al., 2005). Whether there are any PP5 substrates that require PP5 to be in complex with Hsp90 has yet to be determined, but T362 phosphorylation alone is sufficient for high PP5 activity towards *bona fide* substrates, meaning that it can regulate its substrates without having to form a complex with Hsp90 and other Hsp90 co-chaperones (Figure 8D). The fact that PP5 can have activity independent of Hsp90 makes it a better target for treatment as it presents the possibility of targeting misregulated PP5 directly. These findings also open the possibility of controlling many different pathways by targeting a single protein.

Further study into PP5 regulation through PTMs revealed that in addition to its "on switch," PP5 has an "off switch" in the form of ubiquitination. Proteomic data of the PP5 interactome revealed an interaction with the von Hippel-Lindau disease tumor suppressor VHL, which is the substrate recognition component of an E3 ubiquitin ligase complex

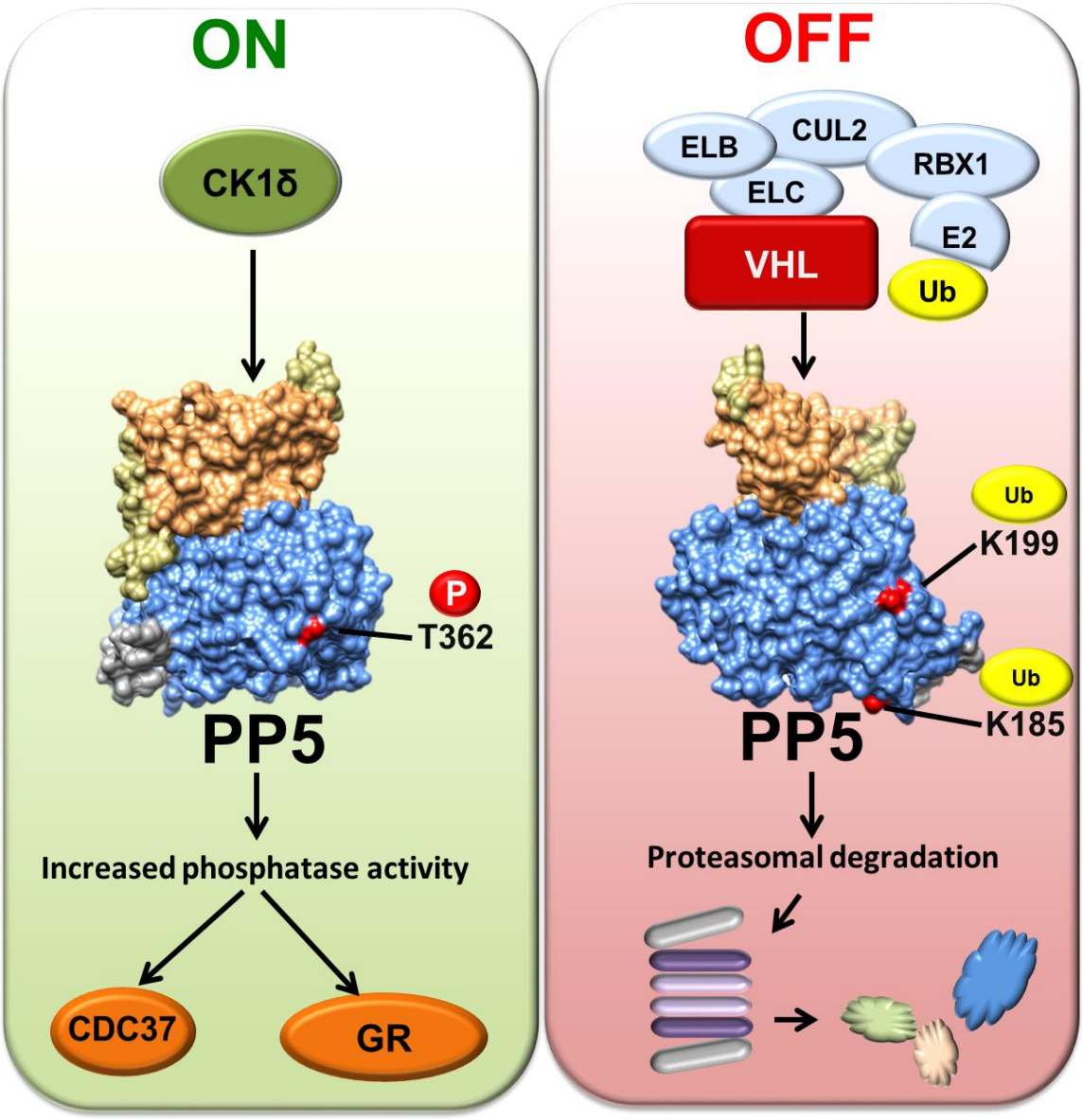


**Figure 21. Post-translational regulation of PP5.**

CK1δ mediated phosphorylation of T362 in the catalytic domain of PP5, activates and enhances its phosphatase activity therefore dephosphorylating its substrates such as the co-chaperone Cdc37 and steroid hormone receptor GR. VCB-Cul2 (VHL-Elongin C-Elongin B-Cullin-2), Rbx1 (E3 ubiquitin ligase) target and ubiquitinate K185 and K199 on PP5. This leads to proteasomal degradation of PP5.

(Table 2). VHL binds and multi mono-ubiquitinates PP5 at two surface residues: K185 and K199 (Figure 10D, 9B-9D). Ubiquitination at these residues ultimately leads to PP5 degradation in the proteasome (Figure 21). These findings have strong implications for the treatment of diseases such as kidney cancer that are linked to VHL mutations. VHL gene mutations are responsible for about 70% of all clear cell renal cell carcinoma (ccRCC) cases, which accounts for the most kidney cancer related deaths as it is the most common form of kidney cancer (Hsieh et al., 2017; Razafinjatovo et al., 2016).

Different mutations of VHL are categorized into four groups: type 1, 2A, 2B, and 2C. Each type of mutation has certain defining characteristics, as well as different risk levels of developing RCC. There are two main differences between type 1 and type 2 mutations. The first is that all type 2 mutations lead to pheochromocytoma development whereas type 1 mutations lack that progression. The second main distinction between types 1 and 2 is that type 1 mutations usually result in premature protein truncations or the complete loss of the protein, whereas type 2 mutations result in missense mutations with various effects on the ability of VHL to regulate its substrates. The difference within type 2 mutations is attributed to the risk level of developing RCC. 2A and 2B are low and high risk for RCC development, respectively. Meanwhile, type 2C mutations do not develop RCC, instead tending to only develop pheochromocytoma (Cowey and Rathmell, 2009).

Patients that have type 1 mutations and lose the expression of full length VHL make up just under half of all ccRCC patients, while type 2 mutations make up an additional 24% of cases (Razafinjatovo et al., 2016). With the lack of functional VHL comes the lack of PP5 regulation as mutated VHL can no longer recognize and ubiquitinate PP5. This leads to the accumulation of PP5, which is then hyperphosphorylated by CK1δ and hyperactive

(Figure 3D). As a result VHL-*null* tumors and tumors with non-functional VHL become accustomed to, and dependent on, increased levels of PP5. Due to the dependence of these tumors on PP5, decrease in PP5 activity leads to cancer cell death.

The *in vivo* data presented in this thesis shows that PP5 knockdown with siRNA results in apoptosis in VHL-null cancer cell lines (786-O and A498), whereas the same treatment has no effect on the VHL-expressing ccRCC Caki-1 cell line (Figures 14B-14C). Furthermore, inhibition of PP5 activity does not need to be direct to kill cancer cells as the inhibition of CK1δ with IC261 results in unphosphorylated and inactive PP5, which ultimately leads to ccRCC cell death (Figures 15-17). The data presented here shows that the observed apoptosis with IC261 treatment is the direct result of PP5 inhibition, and not the result of off-target effects of CK1 inhibition, as overexpression of the phosphomimetic PP5-T362E mutant protected VHL-null cells from apoptosis (Figure 17). Together, these results show that PP5 plays an essential pro-survival role in VHL-null kidney cancers. Therefore, research into specific PP5 inhibitors would open new avenues of treatment for patients with VHL-*null* kidney cancers and any other cancers, such as breast cancer, that require elevated PP5 levels.

Additionally, since the siRNA mediated knockdown of PP5 and the inhibition of its activity (through CK1δ inhibition) leads to the induction of the extrinsic apoptotic pathway as evidenced by the increase in cleaved caspase 8 levels, the work of this thesis suggests an alternative treatment for ccRCC cancers (Figures 18-20). The sensitivity of ccRCC cells to the activation of the extrinsic pathway can potentially be exploited with tumor necrosis factor (TNF)-related apoptosis-inducing ligand (TRAIL) treatment. TRAIL is member of the TNF superfamily, and induces activation of the extrinsic apoptotic

pathway by binding death receptors 4 (DR4) and 5 (DR5) (Allen and El-Deiry, 2012). TRAIL has been tested against many cancers and has been shown to be cytostatic and/or cytotoxic to colon, lung, breast, central nervous system, and melanoma cancers while maintaining low cytotoxicity toward normal cells (Allen and El-Deiry, 2012; Ashkenazi et al., 1999). It may therefore be a promising alternative avenue of cancer treatment for ccRCC, as it may be able to bypass the necessity of PP5 inhibition by activating the extrinsic pathway directly and killing cancer cells more safely.

# Chapter 3 - Materials and Methods

## 3.1 Cell Culture

HEK 293 cells were cultured in DMEM (Dulbecco`s Modified Eagle Media) supplemented with 10% FBS (fetal bovine serum) (Invitrogen). The following three clear cell renal cell carcinoma (ccRCC) cell lines were also used: 786-O, Caki-1, and A498. 786-O cells were cultured in RPMI (Roswell Park Memorial Institute), the Caki-1 cell line was cultured in McCoy's 5A media, and the A498 cells were cultured in MEM (Minimum Essentials Media) supplemented with non-essential amino acids and sodium pyruvate. All three ccRCC cell cultures were also supplemented with 10% FBS.

## 3.2 Transfection

All cells were transfected with individual plasmids using TransIT®-2020 (Mirus) transfection reagent in accordance with the company protocol and incubated at 37ºC for 16 hr. Cells were then kept on ice, washed with cold 1X PBS (Dulbecco's Phosphate Buffered Saline, without calcium or magnesium) (Sigma), and extracted with cold lysis buffer (20 mM Tris (pH 7.5), 100 mM NaCl, 1 mM MgCl2, 0.1% NP40, protease inhibitor cocktail (Roche) and PhosSTOP (Roche)) as previously described (Mollapour et al., 2010; Woodford et al., 2016b). Protein concentration was quantified with 1X Bradford reagent (Biorad).

When indicated, short interfering RNA (siRNA) targeting PP5, HIF1α or Hif2α, obtained from OriGene (SKU: SR303702, SR320469, or SR301415), were transfected in 6-well plates with TransIT®-2020. PP5 knockdown was accomplished using 10nM of each PP5 siRNA duplex (A, B, and C) alongside a 30nM scramble control. Knockdown of HIF1α and HIF2α required 30nM of each HIF siRNA duplex (A, B, and C), and 90nM

control was used for all HIF knockdown experiments. Upon transfection, cells were incubate for 72 hr at 37°C and then extracted at described above.

## 3.3 Mammalian plasmids

N-terminally FLAG tagged human PP5 mammalian expression plasmid pCDNA3.1 and PP5 mutants were derived using by site-directed mutagenesis (Table 3). PP5 was subcloned into bacterial expression plasmid, pRSET-A, containing a $His_6$ tag followed by a PreScission protease site at the N-terminal of human PP5. Site-directed mutagenesis was used to derive indicated PP5 mutants (Table 3). C-terminally tagged CK1δ-cMyc was cloned into pcDNA3.1 (Table 3). N-terminally tagged $VHL_{30}$-FLAG and $VHL_{30}$-$His_6$ were cloned into pcDNA3.1 (Table 3). VHL mutations were either subcloned from HA-VHL Y98H-pRc/CMV or HA-VHL C162F-pRc/CMV constructs purchased from addgene, or performed by site-directed mutagenesis into the $VHL_{30}$-$His_6$ template (Table 3). Mutations were verified by DNA sequencing.

### 3.4 Immunoprecipitation and immunoblotting

For immunoprecipitation and pulldowns, cell lysate was incubated with anti-FLAG antibody conjugated beads (Sigma), or Ni-NTA agarose (Qiagen) for 2 hr at 4ºC for FLAG IPs and $His_6$ pulldowns, respectively. Endogenous IPs of PP5 and VHL were performed by incubating lysate with either the anti-PP5 antibody (2E12, Abcam or Cell signaling), or VHL antibody (3F391, Abcam) for 1 hr followed by a 2 hour incubation with protein G agarose (Invitrogen) at 4ºC. All immunopellets were washed 4 times with cold lysis buffer and either eluted in 5x Laemmli buffer. For purification, immunopellets were washed 4 times with fresh high salt lysis buffer (20 mM HEPES (pH7.0), 500 mM NaCl, 1 mM MgCl2, 0.1% NP40, protease inhibitor cocktail (Roche), and PhosSTOP

(Roche). Proteins bound to Ni-NTA agarose were washed with 50 mM imidazole in lysis buffer (20 mM Tris-HCl (pH 7.5), 100 mM NaCl, protease inhibitor cocktail (Roche), and PhosSTOP (Roche)) and eluted with either 500 mM imidazole in lysis buffer or with 5X Laemmli buffer.

Purified proteins and cell lysates were separated by SDS-PAGE and transferred to a nitrocellulose membrane. The membrane was then blocked with 5% milk, and proteins were detected with indicated antibody dilutions. 1:8000 FLAG, 1:8000 6x-His (ThermoFisher Scientific), 1:8000 Hsp90-835-16F1, 1:8000 GAPDH (ENZO Life Sciences), 1:4000 Cdc37 (StressMarq), 1:2000 GR, 1:1000 p-GR (S211), 1:1000 myc, 1:2000 HA, 1:1000 PP5, 1:4000 Akt, 1:2000 p-Akt (S473), 1:1000 VHL, 1:500 CK1δ, 1:500 CK1ε, 1:1000 cleaved caspase-3, 1:2000 cleaved-PARP, 1:500 HIF1α, 1:500 HI2α, 1:1000 caspase 9, 1:500 caspase 8, 1:1000 cleaved caspase 7 (Cell Signalling), 1:1000 Ubiquitin (Santa Cruz Biotechnology), 1:12000 p-Cdc37 (S13), 1:1000 PP5, 1:1000 VHL(Abcam), 1:1000 phosphothreonine-P6623, 1:1000 phosphoserine-P5747 (Sigma–Aldrich), and 1:10000 GST (GE Healthcare).. Secondary antibodies raised against mouse, rabbit, rat and goat (Santa Cruz Biotechnology) were used at 1:4000 dilution.

### 3.5 Bacterial expression and protein purification

PP5-$His_6$ WT and mutants were expressed and purified from E. coli strain BL21 (DE3). Transformed cells were grown on agar plates containing Luria Broth (LB) with 50 mg/L ampicillin at 37˚C overnight. Colonies were picked and grown in 10 mL of LB + ampicillin overnight. The following day, cultures were diluted to 50 mL with fresh

**Table 3. Primer sequences.**

Restriction sites are underlined, mutated sequences are in red, epitope sequences are in blue, PreScission protease site is in green. Related to Figures 1-6.

| Primer | Sequence |
|---|---|
| Ppt1-Xho1-F(Nat-prom) | ACCTTGGCTCGAGACGAATATGTATTTTATTTTA |
| Ppt1- SpeI-**$His_6$**- R | GGTTATCACTAGTCTA**ATGATGATGATGATGATG**TAAACCAAAAC CACCATTAG |
| Hrr25-HindIII-F | GGACCTGAAGCTTATGGACTTAAGAGTAGGAAGGAAA |
| Hrr25- XhoI-**cMyc**- R | AGTGCTCTCGAGTT**AAAACTCTAAATCTTCTTCGGAGATTAACTTT TGTTCC**AACCAAATTGACTGGCCAGCTGG |
| PP5- Kpn1-**FLAG** | TATGCGGTACC**ATGGATTACAAGGATGACGATGACAAGGGA**GCG GAGGGCGAGAGGACTGAGTGTG |
| PP5-Xho1-R | GGATCGTCTCGAGTCACATCATTCCTAGCTGCAG |
| PP5-Nde1-**$His_6$**-**PreScission**-F | GTAGTCATATGATG**CACCATCATCACCATCA**TCTGGAAGTTCTGT **TCCAGGGGCCC**GCGGAGGGCGAGAGGACTGAGT |
| PP5-T33A-F | AGCGGGCAGAGGAGCTCAAGGCTCAGGCCAATGACTACTTCAA |
| PP5-T33A-R | TTGAAGTAGTCATTGGCCTGAGCCTTGAGCTCCTCTGCCCGCT |
| PP5-T121A-F | CCGCGCTGCGAGACTACGAGGCTGTGGTCAAGGTGAAGCCCCA |
| PP5-T121A-R | TGGGGCTTCACCTTGACCACAGCCTCGTAGTCTCGCAGCGCGG |
| PP5-T171A-F | CGCTGGACATCGAGAGCATGGCTATTGAGGATGAGTACAGCGG |
| PP5-T171A-R | CCGCTGTACTCATCCTCAATAGCCATGCTCTCGATGTCCAGCG |
| PP5-T238A-F | TCAAAGAGACAGAGAAGATTGCTGTATGTGGGGACACCCATGG |
| PP5-T238A-R | CCATGGGTGTCCCCACATACAGCAATCTTCTCTGTCTCTTTGA |
| PP5-T362A-F | TGTTCAGTGAAGACGGTGTCGCTCTGGATGACATCCGGAAAAT |
| PP5-T362A-R | ATTTTCCGGATGTCATCCAGAGCGACACCGTCTTCACTGAACA |
| PP5-T362E-F | TGTTCAGTGAAGACGGTGTCGAACTGGATGACATCCGGAAAAT |
| PP5-T362E-R | ATTTTCCGGATGTCATCCAGTTCGACACCGTCTTCACTGAACA |
| PP5-K32R-F | TGAAGCGGGCAGAGGAGCTCCGTACTCAGGCCAATGACTACTT |
| PP5-K32R-R | AAGTAGTCATTGGCCTGAGTACGGAGCTCCTCTGCCCGCTTCA |
| PP5-K40R-F | CTCAGGCCAATGACTACTTCCGTGCCAAGGACTACGAGAACGC |
| PP5-K40R-R | GCGTTCTCGTAGTCCTTGGCACGGAAGTAGTCATTGGCCTGAG |
| PP5-K185R-F | GACCCAAGCTTGAAGACGGCCGTGTGACAATCAGTTTCATGAA |
| PP5-K185R-R | TTCATGAAACTGATTGTCACACGGCCGTCTTCAAGCTTGGGTC |
| PP5-K199R-F | AGGAGCTCATGCAGTGGTACCGTGACCAGAAGAAACTGCACCG |
| PP5-K199R-R | CGGTGCAGTTTCTTCTGGTCACGGTACCACTGCATGAGCTCCT |
| PP5-K320R-F | ACGGTTTCGAGGGTGAGGTGCGTGCCAAGTACACAGCCCAGAT |
| PP5-K320R-R | ATCTGGGCTGTGTACTTGGCACGCACCTCACCCTCGAAACCGT |
| CK1δ- EcoR1-F | GTCAGCATGAATTCATGGAGCTGAGAGTCGGGAACAG |
| CK1δ- Xho1-**c-Myc**-R | GTTCAGCTCTCGAGTC**AAAACTCTAAATCTTCTTCGGAGATTAAC TTTTGTTC**TCGGTGCACGACAGACTGAAGAC |
| $VHL_{30}$-HindIII-**FLAG**-F | TATGCGAAAGCTTATG**GACTACAAGGACGACGATGACAAG**CCCC GGAGGGCGGAGAACTGGGACGAGGCCGAGGTA |
| $VHL_{30}$-HindIII-**$His_6$**-F | TATGCGAAAGCTTATG**CATCATCACCACCATCAC**CCCCGGAGGG CGGAGAACTGG |
| $VHL_{30}$-Xho1-R | AGTGCGCTCTCGAGTCAATCTCCCATCCGTTGATGT |

LB+ amplicilin and grown with continuous 200 RPM shaking at 37˚C until OD600 = 0.6. The cultures were then cooled to 30˚C and induced with 100 mg/L IPTG until OD600 = 1.2. Cells were harvested by centrifugation and lysed by sonication in fresh lysis buffer without detergent (20 mM Tris (pH 7.5), 100 mM NaCl, 1 mM MgCl2, protease inhibitor cocktail (Roche) and PhosSTOP (Roche)). Supernatant was collected and PP5-$His_6$ expression was assessed by immunoblotting. Purification of PP5-$His_6$ was carried out by two sequential Ni-NTA agarose (Qiagen) pulldowns, followed by imidazole competition after each pulldown (see above). The pure protein was then washed and concentrated in a 30K Amicon® Ultra, 500 µL centrifugal filter unit (Millipore) with lysis buffer 3 times. Concentrations were determined by the Micro BCA™ Protein Assay Kit (Thermo Scientific) as per manual protocol. Then, 50 ng of the purified proteins were run on an SDS-PAGE gel and coomassie stained to confirm purity prior to use in assays.

### 3.6 *In vitro* kinase assay

Wild-type human PP5 and its non-phospho-T362A-mutant were N-terminally $His_6$ tagged using pRSETA plasmid for bacterial expression. PP5 and its phospho-mutant were isolated by incubating 2 mg of protein extracts with 50 µl of Ni-NTA agarose (Qiagen) for 2 hr. The Ni-NTA agarose beads were washed with 30 µM imidazole and then incubated with 20ng of baculovirus expressed and purified active CK1δ-GST or CK1ε-GST (SignalChem). The assay was carried out in 50 mM Tris-HCl (pH 7.5), 10 mM $MgCl_2$ and 0.2 mM ATP for 15 min at 30˚C. The Ni-NTA agarose beads were washed twice with 30 µM imidazole and then eluted with 300 µM imidazole. Samples were then dialyzed with Amicon Ultra-0.5 centrifugal filter unit with Ultracel-30 membrane (Millipore), quantified and then analyzed by immunoblotting with anti-hexahistidine (Thermo Scientific), pan-

anti-phosphothreonine-P6623 (Sigma-Aldrich), anti-phospho-serine-P5754 (Sigma-Aldrich), and anti-GST (GE Healthcare) antibodies.

### 3.7 *In vitro* Cdc37 dephosphorylation assay

Rate of PP5 dephosphorylation of S13-Cdc37 was monitored by mixing 5 μM purified phospho-S13-Cdc37 with and without 2.5 μM Hsp90α in a buffer containing 100 mM NaCl, 50 mMTris, pH7.5, 2 mM DTT, and 1 mM $MnCl_2$. 0.25 μM of purified PP5 (wild-type, phospho-mutants, or CK1δ phosphorylated) was added to start the reaction. The samples were incubated at 30°C with time points taken every 10 min for SDS/PAGE analysis. The phosphorylation state of S13-Cdc37 was examined by immunoblotting using phospho-Ser13–specific antibody (Abcam).

### 3.8 PP5 activity assay with pNPP

PP5 activity was assayed by monitoring the colorimetric change of the reaction caused by the hydrolysis of the non-specific phosphatase substrate, *para*-Nitrophenyl Phosphate, pNPP. Samples were assayed in 96-well plate in triplicate. Proteins were incubated together at 30°C for 30 minutes prior to addition of indicated amount of pNPP substrate. Each well contained 0.15 μM PP5-$His_6$ WT or mutant and, when indicated, 1.5 μM Hsp90α (proteins were purified into a buffer containing 0.5 mM $MnCl_2$, 50 mM NaCl and 100 mM Tris, pH 8.0). Upon the addition of substrate, the absorbance was measured at 405 nm over 10 minutes at 30 °C. Data is presented as a kinetic curve of absorbance over time (seconds). Fold change in PP5 activity was calculated from the final data point of each curve (30 mM pNPP substrate) relative to WT PP5 in the absence of Hsp90α.

### 3.9 *In vitro* ubiquitination of PP5

50 ng WT-PP5-$His_6$ or the K185R/K199R-PP5-$His_6$ mutant were bound to Ni-NTA agarose and incubated with VHL complex (Millipore), in a buffer containing 25 mM MOPS pH7.5, 0.01% Tween 20, 5 mM MgCl2, 10 μM ATP, 1 ng RBX1 (Millipore). The reaction was initiated with the addition of 2ng GST-ubiquitin, and incubated for 30 minutes at 30˚C. After 30 minutes, the Ni-NTA agarose was washed with lysis buffer, resuspended in 5X Laemmli buffer, boiled, separated by SDS-PAGE and transferred to nitrocellulose membranes. Ubiquitination was detected with by immunoblotting using an anti-ubiquitin antibody (Santa Cruz Biothech).

### 3.10 Analysis of human ccRCC tumors

Tumor and adjacent normal tissue samples of patients with conventional ccRCC were obtained with informed written consent from the Department of Urology at SUNY Upstate Medical University. ccRCC patient tumor samples were dissected into approximately 8 $mm^3$ pieces at the time of radical or partial nephrectomy, which was done with less than 10 minutes of renal ischemia. Protein was then extracted from the tissue and quantified as previously described (Woodford et al., 2016b). Normal and tumor tissue samples were also stained with haematoxylin and eosin (H&E) and were examined by a pathologist.

### 3.11 Drug Treatments

Caki-1, 786-O and A498 cells were cultured until 60% confluency and treated with different concentrations of CK1δ inhibitor IC261 for 16 hr. Cells were then extracted and immunoblotted as described above. Z-VAD-fmk treated cells were treated with 10μM z-VAD-fmk or DMSO control for 1 hour prior to the addition of IC261, for a total of 17 hour

z-VAD-fmk and 16 hour IC261 treatment. Cells were then extracted as described and immunoblotted for apoptotic markers.

### 3.12 Annexin V/PI Apoptosis Analysis

Apoptosis was detected by Annexin V/PI immunostaining. Caki-1, 786-O and A498 cells were cultured in complete medium until 80% confluency and different concentrations of CK1δ inhibitor IC261 were added in the culture medium. Cells were then stained with Annexin-V-FITC and propidium iodine (PI) using the Apoptosis Detection Kit (BioRad/AbD Serotec) in accordance with the manufacturers' protocol. Percentage of unstained negative (-), single stained early apoptotic cells Annexin V-FITC positive (+), PI positive (+) necrotic cells, double positive Annexin V-FITC (+)/PI (+) late apoptotic/necrotic and total apoptotic cells (Annexin V+/PI±) at 24hrs post treatment was determined by flow cytometry. Fluorescence was measured immediately using LSRFORTESSA (BD) collected from 10,000 events and analysis was performed using FlowJo software.

### 3.13 MTT Assay

MTT assay was performed as described in the Quick Cell Proliferation Colorimetric Assay Kit Plus (BioVision, Cat# K302-500). A498, 786-O and Caki-1 cells were plated at 10,000 cells per well in 96-well plates. Cells were treated with 0.1, 0.2, 0.5, 1.0 and 2.0 µM IC261. After 72 hr, 10µl WST reagent was added to each well and returned to the 37°C incubator for 1 hour. Subsequently, the absorbance at 450nm was measured on a Tecan Infinite M200 Pro and proliferation rate was calculated. For transfected cells, transfections were incubated for 48 hr prior to trypsinization and plating in the 96-well plate.

### 3.14 Soft Agar Colony Formation Assay

Soft agar colony formation assay was performed similar to previously described method (Borowicz et al., 2014). In brief, 1.2% and 2% agar was dissolved in deionized water, autoclaved, and cooled to 42°C in an equilibrated water bath. To prepare the bottom layer, 1.5 ml of 1:1 mixture of 2% agar and tissue culture medium was plated into each well of a 6-well plate and allowed to solidify. To plate 5,000 Caki-1, A498 and 786-O cells/well, sub-confluent cells were trypsinized, counted and re-suspended to an approximate concentration of 6,667 cells/ml. The cells were then aliquoted into six tubes, and the appropriate concentration of IC261 or DMSO was added to each aliquot. To prepare the top layer, 1.5ml of a 1:1 mixture of 1.2% agar and cultured cells (at 6,667 cells/ml) were plated into each well of a 6-well plate on top of the bottom layer. Upon solidification, the plates were maintained in a 37°C incubator at 5% $CO_2$. Twice weekly, 100µl of culture media was added to the top layer to prevent desiccation. After 21 days, plates were imaged on a Nikon Ci-L microscope for two observers equipped with an IDEA camera using SPOT software.

### 3.15 Mass spectrometry analysis

Visible bands were excised from the gel manually and cut into small pieces approximately 1 mm x 1 mm. These gel pieces were destained using 1:1 30 mM potassium ferricyanide and 100 mM sodium thiosulfate for 10 minutes. The destained gel pieces were then washed with 25 mM ammonium bicarbonate and acetonitrile alternatively for 5 minutes each wash. This alternating wash cycle was repeated 3 times. The gel pieces were then dehydrated in 100% acetonitrile. After removing all acetonitrile, 25 µl of porcine trypsin (Promega) dissolved in 25 mM ammonium bicarbonate at a concentration of 4

µg/ml was added to the gel pieces. The gel pieces were then kept at room temperature overnight (approximately 12-16 hr). Following the overnight digestion, the supernatant was transferred to a second tube and acetonitrile was added to the gel pieces to complete the extraction of digested peptides. This extract was added to the first supernatant and this combined solution, containing the extracted peptides was frozen and lyophilized. The peptides were resuspended in 5 µl of 100:99:1 acetonitrile: water: trifluoroacetic acid immediately prior to spotting on the MALDI target. For MALDI analysis, the matrix solution consisted of alpha-cyano-4-hydroxycinnamic acid (Aldrich Chemical Co. Milwaukee, WI) saturating a solution of 1:1:0.01 acetonitrile: 25 mM ammonium citrate: trifuoroacetic acid. Approximately 0.15 µl of peptide solution was spotted on the MALDI target immediately followed by 0.15 µl of the matrix solution. This combined solution was allowed to dry at room temperature. MALDI MS and MS/MS data was then acquired using the ABSCIEX TOF/TOF® 5800 Mass Spectrometer. Resultant peptide mass fingerprint and peptide sequence data was submitted to the UniProt database using the Mascot search engine to which relevance is calculated and scores are displayed. Data are presented in (Table 2).

### 3.16 Quantification and statistical analysis

The data presented are the representative or examples of three biological replicates unless otherwise specified. Data were analyzed with the unpaired *t*-test. Asterisks in figures indicate significant differences (* $P < 0.05$, ** $P < 0.005$, *** $P < 0.0005$, and **** $P < 0.0001$). Error bars represent the standard deviation (S.D.) for three independent experiments, unless otherwise indicated.

# References


Ali, A., Zhang, J., Bao, S., Liu, I., Otterness, D., Dean, N.M., Abraham, R.T., and Wang, X.F. (2004). Requirement of protein phosphatase 5 in DNA-damage-induced ATM activation. Genes Dev *18*, 249-254.

Allen, J.E., and El-Deiry, W.S. (2012). Regulation of the human TRAIL gene. Cancer Biol Ther *13*, 1143-1151.

Amable, L., Grankvist, N., Largen, J.W., Ortsater, H., Sjoholm, A., and Honkanen, R.E. (2011). Disruption of serine/threonine protein phosphatase 5 (PP5:PPP5c) in mice reveals a novel role for PP5 in the regulation of ultraviolet light-induced phosphorylation of serine/threonine protein kinase Chk1 (CHEK1). J Biol Chem *286*, 40413-40422.

Ardito, F., Giuliani, M., Perrone, D., Troiano, G., and Lo Muzio, L. (2017). The crucial role of protein phosphorylation in cell signaling and its use as targeted therapy International Journal of Molecular Medicine *40*, 271-280.

Ashkenazi, A., Pai, R.C., Fong, S., Leung, S., Lawrence, D.A., Marsters, S.A., Blackie, C., Chang, L., McMurtrey, A.E., Hebert, A., *et al.* (1999). Safety and antitumor activity of recombinant soluble Apo2 ligand. J Clin Invest *104*, 155-162.

Borowicz, S., Van Scoyk, M., Avasarala, S., Karuppusamy Rathinam, M.K., Tauler, J., Bikkavilli, R.K., and Winn, R.A. (2014). The soft agar colony formation assay. J Vis Exp, e51998.

Bouazza, B., Krytska, K., Debba-Pavard, M., Amrani, Y., Honkanen, R.E., Tran, J., and Tliba, O. (2012). Cytokines alter glucocorticoid receptor phosphorylation in airway cells: role of phosphatases. Am J Respir Cell Mol Biol *47*, 464-473.

Chen, Y.L., Hung, M.H., Chu, P.Y., Chao, T.I., Tsai, M.H., Chen, L.J., Hsiao, Y.J., Shih, C.T., Hsieh, F.S., and Chen, K.F. (2017). Protein phosphatase 5 promotes hepatocarcinogenesis through interaction with AMP-activated protein kinase. Biochem Pharmacol *138*, 49-60.

Cohen, P. (2001). The role of protein phosphorylation in human health and disease. The Sir Hans Krebs Medal Lecture. Eur J Biochem *268*, 5001-5010.

Cowey, C.L., and Rathmell, W.K. (2009). VHL Gene Mutations in Renal Cell Carcinoma: Role as a Biomarker of Disease Outcome and Drug Efficacy. Current Oncology Reports *11*, 94–101.

Das, A.K., Cohen, P.W., and Barford, D. (1998). The structure of the tetratricopeptide repeats of protein phosphatase 5: implications for TPR-mediated protein-protein interactions. EMBO J *17*, 1192-1199.

Davies, T.H., Ning, Y.M., and Sanchez, E.R. (2005). Differential control of glucocorticoid receptor hormone-binding function by tetratricopeptide repeat (TPR) proteins and the immunosuppressive ligand FK506. Biochemistry *44*, 2030-2038.

Dushukyan, N., Dunn, D.M., Sager, R.A., Woodford, M.R., Loiselle, D.R., Daneshvar, M., Baker-Williams, A.J., Chisholm, J.D., Truman, A.W., Vaughan, C.K., et al. (2017). Phosphorylation and Ubiquitination Regulate Protein Phosphatase 5 Activity and Its Prosurvival Role in Kidney Cancer. Cell Rep 21, 1883-1895.

Fernandez, S.V., Russo, I.H., and Russo, J. (2006). Estradiol and its metabolites 4-hydroxyestradiol and 2-hydroxyestradiol induce mutations in human breast epithelial cells. Int J Cancer *118*, 1862-1868.

Flotow, H., Graves, P.R., Wang, A.Q., Fiol, C.J., Roeske, R.W., and Roach, P.J. (1990). Phosphate groups as substrate determinants for casein kinase I action. J Biol Chem *265*, 14264-14269.

Gentile, S., Darden, T., Erxleben, C., Romeo, C., Russo, A., Martin, N., Rossie, S., and Armstrong, D.L. (2006). Rac GTPase signaling through the PP5 protein phosphatase. PNAS *103*, 5202–5206.

Ghobrial, I.M., McCormick, D.J., Kaufmann, S.H., Leontovich, A.A., Loegering, D.A., Dai, N.T., Krajnik, K.L., Stenson, M.J., Melhem, M.F., Novak, A.J., *et al.* (2005). Proteomic analysis of mantle-cell lymphoma by protein microarray. Blood *105*, 3722-3730.

Golden, T., Aragon, I.V., Rutland, B., Tucker, J.A., Shevde, L.A., Samant, R.S., Zhou, G., Amable, L., Skarra, D., and Honkanen, R.E. (2008a). Elevated levels of Ser/Thr protein phosphatase 5 (PP5) in human breast cancer. Biochim Biophys Acta *1782*, 259-270.

Golden, T., Swingle, M., and Honkanen, R.E. (2008b). The role of serine/threonine protein phosphatase type 5 (PP5) in the regulation of stress-induced signaling networks and cancer. Cancer Metastasis Rev *27*, 169-178.

Gossage, L., Eisen, T., and Maher, E.R. (2015). VHL, the story of a tumour suppressor gene. Nat Rev Cancer *15*, 55-64.

Haslbeck, V., Eckl, J.M., Drazic, A., Rutz, D.A., Lorenz, O.R., Zimmermann, K., Kriehuber, T., Lindemann, C., Madl, T., and Richter, K. (2015). The activity of protein phosphatase 5 towards native clients is modulated by the middle- and C-terminal domains of Hsp90. Sci Rep *5*, 17058.

Hinds, T.D., Jr., and Sanchez, E.R. (2008). Protein phosphatase 5. Int J Biochem Cell Biol *40*, 2358-2362.

Hsieh, J.J., Purdue, M.P., Signoretti, S., Swanton, C., Albiges, L., Schmidinger, M., Heng, D.Y., Larkin, J., and Ficarra, V. (2017). Renal cell carcinoma. Nature Reviews Disease Primers *3*, 17009.

Ikeda, K., Ogawa, S., Tsukui, T., Horie-Inoue, K., Ouchi, Y., Kato, S., Muramatsu, M., and Inoue, S. (2004). Protein phosphatase 5 is a negative regulator of estrogen receptor-mediated transcription. Mol Endocrinol *18*, 1131-1143.

Iliopoulos, O., Kibel, A., Gray, S., and Kaelin, W.G., Jr. (1995). Tumour suppression by the human von Hippel-Lindau gene product. Nat Med *1*, 822-826.

Jacob, W., Rosenzweig, D., Vazquez-Martin, C., Duce, S.L., and Cohen, P.T. (2015). Decreased adipogenesis and adipose tissue in mice with inactivated protein phosphatase 5. Biochem J *466*, 163-176.

Kamura, T., Koepp, D.M., Conrad, M.N., Skowyra, D., Moreland, R.J., Iliopoulos, O., Lane, W.S., Kaelin, W.G., Jr., Elledge, S.J., Conaway, R.C., *et al.* (1999). Rbx1, a component of the VHL tumor suppressor complex and SCF ubiquitin ligase. Science *284*, 657-661.

Kamura, T., Sato, S., Iwai, K., Czyzyk-Krzeska, M., Conaway, R.C., and Conaway, J.W. (2000). Activation of HIF1alpha ubiquitination by a reconstituted von Hippel-Lindau (VHL) tumor suppressor complex. Proc Natl Acad Sci U S A *97*, 10430-10435.

Liehr, J.G. (2000). Is estradiol a genotoxic mutagenic carcinogen? Endocrine Reviews *21*, 40-54.

Lubert, E.J., Hong, Y., and Sarge, K.D. (2001). Interaction between protein phosphatase 5 and the A subunit of protein phosphatase 2A: evidence for a heterotrimeric form of protein phosphatase 5. J Biol Chem *276*, 38582-38587.

Mayer, M.P., and Le Breton, L. (2015). Hsp90: breaking the symmetry. Mol Cell *58*, 8-20.

Mazalouskas, M.D., Godoy-Ruiz, R., Weber, D.J., Zimmer, D.B., Honkanen, R.E., and Wadzinski, B.E. (2014). Small G proteins Rac1 and Ras regulate serine/threonine protein phosphatase 5 (PP5).extracellular signal-regulated kinase (ERK) complexes involved in the feedback regulation of Raf1. J Biol Chem *289*, 4219-4232.

Meeusen, B., and Janssens, V. (2018). Tumor suppressive protein phosphatases in human cancer: Emerging targets for therapeutic intervention and tumor stratification. Int J Biochem Cell Biol *96*, 98-134.

Mollapour, M., Tsutsumi, S., Donnelly, A.C., Beebe, K., Tokita, M.J., Lee, M.J., Lee, S., Morra, G., Bourboulia, D., Scroggins, B.T., *et al.* (2010). Swe1Wee1-dependent tyrosine phosphorylation of Hsp90 regulates distinct facets of chaperone function. Mol Cell *37*, 333-343.

Morita, K., Saitoh, M., Tobiume, K., Matsuura, H., Enomoto, S., Nishitoh, H., and Ichijo, H. (2001). Negative feedback regulation of ASK1 by protein phosphatase 5 (PP5) in response to oxidative stress. EMBO J *20*, 6028-6036.

Oberoi, J., Dunn, D.M., Woodford, M.R., Mariotti, L., Schulman, J., Bourboulia, D., Mollapour, M., and Vaughan, C.K. (2016). Structural and functional basis of protein phosphatase 5 substrate specificity. Proc Natl Acad Sci U S A *113*, 9009-9014.

Ollendorff, V., and Donoghue, D.J. (1997). The serine/threonine phosphatase PP5 interacts with CDC16 and CDC27, two tetratricopeptide repeat-containing subunits of the anaphase-promoting complex. J Biol Chem *272*, 32011-32018.

Partch, C.L., Shields, K.F., Thompson, C.L., Selby, C.P., and Sancar, A. (2006). Posttranslational regulation of the mammalian circadian clock by cryptochrome and protein phosphatase 5. Proc Natl Acad Sci U S A *103*, 10467-10472.

Periyasamy, S., Warrier, M., Tillekeratne, M.P., Shou, W., and Sanchez, E.R. (2007). The immunophilin ligands cyclosporin A and FK506 suppress prostate cancer cell growth by androgen receptor-dependent and -independent mechanisms. Endocrinology *148*, 4716-4726.

Razafinjatovo, C., Bihr, S., Mischo, A., Vogl, U., Schmidinger, M., Moch, H., and Schraml, P. (2016). Characterization of VHL missense mutations in sporadic clear cell renal cell carcinoma: hotspots, affected binding domains, functional impact on pVHL and therapeutic relevance. BMC Cancer *16*, 638.

Sanchez, E.R. (2012). Chaperoning steroidal physiology: lessons from mouse genetic models of Hsp90 and its cochaperones. Biochim Biophys Acta *1823*, 722-729.

Schittek, B., and Sinnberg, T. (2014). Biological functions of casein kinase 1 isoforms and putative roles in tumorigenesis. Mol Cancer *13*, 231.

Schopf, F.H., Biebl, M.M., and Buchner, J. (2017). The HSP90 chaperone machinery. Nat Rev Mol Cell Biol *18*, 345-360.

Schulke, J.P., Wochnik, G.M., Lang-Rollin, I., Gassen, N.C., Knapp, R.T., Berning, B., Yassouridis, A., and Rein, T. (2010). Differential impact of tetratricopeptide repeat proteins on the steroid hormone receptors. PLoS One *5*, e11717.

Shao, J., Hartson, S.D., and Matts, R.L. (2002). Evidence That Protein Phosphatase 5 Functions To Negatively Modulate the Maturation of the Hsp90-Dependent Heme-Regulated eIF2R Kinase. Biochemistry *41*, 6770-6779.

Shi, Y. (2009). Serine/threonine phosphatases: mechanism through structure. Cell *139*, 468-484.

Silverstein, A.M., Galigniana, M.D., Chen, M.-S., Owens-Grillo, J.K., Chinkers, M., and B., P.W. (1997). Protein Phosphatase 5 Is a Major Component of Glucocorticoid Receptor-hsp90 Complexes with Properties of an FK506-binding Immunophilin. Journal of Biological Chemistry *272*, 16224–16230.

Stebbins, C.E., Kaelin, W.G., Jr., and Pavletich, N.P. (1999). Structure of the VHL-ElonginC-ElonginB complex: implications for VHL tumor suppressor function. Science *284*, 455-461.

Stechschulte, L.A., Ge, C., Hinds, T.D., Jr., Sanchez, E.R., Franceschi, R.T., and Lecka-Czernik, B. (2016). Protein Phosphatase PP5 Controls Bone Mass and the Negative Effects of Rosiglitazone on Bone through Reciprocal Regulation of PPARgamma (Peroxisome Proliferator-activated Receptor gamma) and RUNX2 (Runt-related Transcription Factor 2). J Biol Chem *291*, 24475-24486.

Swingle, M.R., Honkanen, R.E., and Ciszak, E.M. (2004). Structural basis for the catalytic activity of human serine/threonine protein phosphatase-5. J Biol Chem *279*, 33992-33999.

Tomsig, J.L., Snyder, S.L., and Creutz, C.E. (2003). Identification of targets for calcium signaling through the copine family of proteins. Characterization of a coiled-coil copine-binding motif. J Biol Chem *278*, 10048-10054.

Vaughan, C.K., Mollapour, M., Smith, J.R., Truman, A., Hu, B., Good, V.M., Panaretou, B., Neckers, L., Clarke, P.A., Workman, P., *et al.* (2008). Hsp90-dependent activation of protein kinases is regulated by chaperone-targeted dephosphorylation of Cdc37. Mol Cell *31*, 886-895.

von Kriegsheim, A., Pitt, A., Grindlay, G.J., Kolch, W., and Dhillon, A.S. (2006). Regulation of the Raf-MEK-ERK pathway by protein phosphatase 5. Nat Cell Biol *8*, 1011-1016.

Walton-Diaz, A., Khan, S., Bourboulia, D., Trepel, J.B., Neckers, L., and Mollapour, M. (2013). Contributions of co-chaperones and post-translational modifications towards Hsp90 drug sensitivity. Future Med Chem *5*, 1059-1071.

Wandinger, S.K., Suhre, M.H., Wegele, H., and Buchner, J. (2006). The phosphatase Ppt1 is a dedicated regulator of the molecular chaperone Hsp90. EMBO J *25*, 367-376.

Wang, J., Zhu, J., Dong, M., Yu, H., Dai, X., and Li, K. (2015). Inhibition of protein phosphatase 5 (PP5) suppresses survival and growth of colorectal cancer cells. Biotechnol Appl Biochem *62*, 621-627.

Wang, Z., Chen, W., Kono, E., Dang, T., and Garabedian, M.J. (2007). Modulation of glucocorticoid receptor phosphorylation and transcriptional activity by a C-terminal-associated protein phosphatase. Mol Endocrinol *21*, 625-634.

Wechsler, T., Chen, B.P., Harper, R., Morotomi-Yano, K., Huang, B.C., Meek, K., Cleaver, J.E., Chen, D.J., and Wabl, M. (2004). DNA-PKcs function regulated specifically by protein phosphatase 5. Proc Natl Acad Sci U S A *101*, 1247-1252.

Woodford, M.R., Dunn, D., Miller, J.B., Jamal, S., Neckers, L., and Mollapour, M. (2016a). Impact of Posttranslational Modifications on the Anticancer Activity of Hsp90 Inhibitors. Adv Cancer Res *129*, 31-50.

Woodford, M.R., Truman, A.W., Dunn, D.M., Jensen, S.M., Cotran, R., Bullard, R., Abouelleil, M., Beebe, K., Wolfgeher, D., Wierzbicki, S., *et al.* (2016b). Mps1 Mediated Phosphorylation of Hsp90 Confers Renal Cell Carcinoma Sensitivity and Selectivity to Hsp90 Inhibitors. Cell Rep *14*, 872-884.

Wu, L., Zhang, J., Wu, H., and Han, E. (2015). DNA-PKcs interference sensitizes colorectal cancer cells to a mTOR kinase inhibitor WAY-600. Biochem Biophys Res Commun *466*, 547-553.

Xu, W., Mollapour, M., Prodromou, C., Wang, S., Scroggins, B.T., Palchick, Z., Beebe, K., Siderius, M., Lee, M.J., Couvillon, A., *et al.* (2012). Dynamic tyrosine phosphorylation modulates cycling of the HSP90-P50(CDC37)-AHA1 chaperone machine. Mol Cell *47*, 434-443.

Xu, X., Lagercrantz, J., Zickert, P., Bajalica-Lagercrantz, S., and Zetterberg, A. (1996). Chromosomal localization and 5' sequence of the human protein serine/threonine phosphatase 5' gene. Biochem Biophys Res Commun *218*, 514-517.

Yamaguchi, Y., Katoh, H., Mori, K., and Negishi, M. (2002). G(alpha)12 and G(alpha)13 Interact with Ser/Thr Protein Phosphatase Type 5 and Stimulate Its Phosphatase Activity. Current Biology *12*, 1353–1358.

Yang, J., Roe, S.M., Cliff, M.J., Williams, M.A., Ladbury, J.E., Cohen, P.T., and Barford, D. (2005). Molecular basis for TPR domain-mediated regulation of protein phosphatase 5. EMBO J *24*, 1-10.

Yue, W., Yager, J.D., Wang, J.P., Jupe, E.R., and Santen, R.J. (2013). Estrogen receptor-dependent and independent mechanisms of breast cancer carcinogenesis. Steroids *78*, 161-170.

Zeke, T., Morrice, N., Vazquez-Martin, C., and Cohen, P.T.W. (2005). Human protein phosphatase 5 dissociates from heat-shock proteins and is proteolytically activated in response to arachidonic acid and the microtubule-depolymerizing drug nocodazole. Biochemical Journal *385*, 45-56.

Zhang, J., Bao, S., Furumai, R., Kucera, K.S., Ali, A., Dean, N.M., and Wang, X.F. (2005). Protein phosphatase 5 is required for ATR-mediated checkpoint activation. Mol Cell Biol *25*, 9910-9919.

Zhang, Y., Leung, D.Y., Nordeen, S.K., and Goleva, E. (2009). Estrogen inhibits glucocorticoid action via protein phosphatase 5 (PP5)-mediated glucocorticoid receptor dephosphorylation. J Biol Chem *284*, 24542-24552.

Zhao, S., and Sancar, A. (1997). Human Blue-light Photoreceptor hCRY2 Specifically Interacts with Protein Serinemhreonine Phosphatase 5 and Modulates Its Activity. Photochemistry and Photobiology *66*, 727-731.

Zhou, G., Golden, T., Aragon, I.V., and Honkanen, R.E. (2004). Ser/Thr protein phosphatase 5 inactivates hypoxia-induced activation of an apoptosis signal-regulating kinase 1/MKK-4/JNK signaling cascade. J Biol Chem *279*, 46595-46605.

Zuo, Z., Dean, N.M., and Honkanen, R.E. (1998). Serine/Threonine Protein Phosphatase Type 5 Acts Upstream of p53 to Regulate the Induction of p21WAF1/Cip1 and Mediate Growth Arrest. Journal of Biological Chemistry *273*, 12250–12258.

Zuo, Z., Urban, G., Scammell, J.G., Dean, N.M., McLean, T.K., Aragon, I., and Honkanen, R.E. (1999). Ser/Thr protein phosphatase type 5 (PP5) is a negative regulator of glucocorticoid receptor-mediated growth arrest. Biochemistry *38*, 8849-8857.